

# Interacting Crystalline Topological Insulators in two-dimensions with Time-Reversal Symmetry

Martina O. Soldini,<sup>1</sup> Ömer M. Aksoy,<sup>2</sup> and Titus Neupert<sup>1</sup>

<sup>1</sup>*Department of Physics, University of Zurich, Winterthurerstrasse 190, CH-8057 Zürich, Switzerland*

<sup>2</sup>*Department of Physics, Massachusetts Institute of Technology, Cambridge, Massachusetts 02139, USA*

Topology is routinely used to understand the physics of electronic insulators. However, for strongly interacting electronic matter, such as Mott insulators, a comprehensive topological characterization is still lacking. When their ground state only contains short range entanglement and does not break symmetries spontaneously, they generically realize crystalline fermionic symmetry protected topological phases (cFSPTs), supporting gapless modes at the boundaries or at the lattice defects. Here, we provide an exhaustive classification of cFSPTs in two-dimensions with U(1) charge-conservation and spinful time-reversal symmetries, namely those generically present in spin-orbit coupled insulators, for any of the 17 wallpaper groups. It has been shown that the classification of cFSPTs can be understood from appropriate real-space decorations of lower-dimensional subspaces, and we expose how these relate to the Wyckoff positions of the lattice. We find that all nontrivial one-dimensional decorations require electronic interactions. Furthermore, we provide model Hamiltonians for various decorations, and discuss the signatures of cFSPTs. This classification paves the way to further explore topological interacting insulators, providing the backbone information in generic model systems and ultimately in experiments.

## I. INTRODUCTION

A rich set of phases can be found in electronic crystalline materials when interactions are preeminent. Among these possibilities, a prime example is that of the fermionic symmetry protected topological (FSPT) phases of matter. An FSPT phase is characterized by the existence of a bulk gap accompanied by robust gapless boundary states, which can only be gapped when the protecting symmetries are broken. Two distinct FSPT phases cannot be connected by continuously changing the parameters of the Hamiltonian, unless a gap closing or symmetry breaking transition occurs. As opposed to intrinsically topologically ordered systems, ground states of FSPTs contain only short range entanglement.

A classification of *noninteracting* FSPT phases, such as band insulators and superconductors, has been achieved in the 10-fold way [1–3], where 10 symmetry classes are defined depending on whether or not the single-particle Hamiltonians are symmetric under charge-conjugation symmetry, time-reversal symmetry (TRS), or a combination of the two. Over the years, weakly interacting electronic materials showcasing some of the boundary modes predicted by the 10-fold way have been discovered: the paradigmatic examples include <sup>1</sup> the quantum spin Hall

effect [7–9], and the observation of gapless surface states in three-dimensional topological insulators [10, 11].

In the 10-fold way, the gapless boundary modes are protected by internal symmetries alone. However, the underlying lattice structure of crystalline matter naturally provides more symmetries such as translations, rotations, spatial inversion, or mirror operations. These symmetries enrich the known classification of FSPT phases by providing protection to distinct gapless boundary modes, which become gappable if the symmetry is broken. The corresponding phases are called *crystalline* FSPT (cFSPT) phases. Early examples of noninteracting cFSPT have been obtained by extending the 10-fold way with crystalline symmetries [12–24], which led to the discovery of novel phases such as higher order topological phases [25–29]. A milestone in this direction was the development of the comprehensive frameworks of symmetry indicators [30, 31] and topological quantum chemistry [32–36], which allowed to characterize entire material databases. Since then, some of these phases have been observed in insulating electronic materials [37–41] and insulating or superconducting metamaterials [42–44].

In the last decade, it has been realized that interaction effects can drastically change the classification of FSPTs, as well as cFSPTs. Following the seminal works of Fidkowski and Kitaev [45, 46], several works have shown that the classification of FSPTs (and cFSPTs) can be reduced due to the presence of interactions [47–57]. In other words, nontrivial cFSPT phases may be connected to the trivial one by interaction terms. Parallel to these efforts, bosonic and fermionic SPT phases have been classified using the tools of algebraic topology such as cohomology and cobordism groups [6, 58–68]. In addition to reducing the noninteracting classification, interactions may also enhance the FSPT classification leading to *intrinsically interacting* phases that do not admit noninteracting counterparts [6, 65, 69–73].

<sup>1</sup> The integer quantum Hall (IQH) states [4], while being the first realizations of fermionic topological phases of matter, are not protected by any symmetries owing to the fact that their gapless chiral boundary modes cannot be gapped even when all the symmetries are broken. IQH states are examples of *invertible* topological phases that are not SPT phases. These states carry long-range entanglement but do not support any nontrivial anyonic excitations [5]. The low-energy properties of invertible topological phases (SPT or not) are described by the so-called invertible topological field theories [6].

A breakthrough in classifying interacting cFSPTs has been achieved when a correspondence between topological phases with crystalline symmetries and internal symmetries was uncovered in Refs. 74 and 75 in the form of the so-called *crystalline equivalence principle* (see also Refs. 76 and 77). This correspondence can be understood from decorating points, lines, and planes in space with FSPTs through the so-called *real-space construction* [78–85].

Despite the widespread presence of interactions in real electronic materials, the experimental realization and observation of interacting cFSPT phases have so far remained elusive, while some of them have been realized in cold atom experiments [86, 87]. A particularly relevant case is that of generic interacting electronic insulating materials with spin-orbit coupling and TRS. These properties encompass a range of materials, such as non-magnetic Mott insulators. In the language of the 10-fold way, such electronic insulators belong to the class AII, for which the relevant symmetries are U(1) charge-conservation and spinful TRS.

The classification of crystalline bosonic symmetry protected topological (SPT) states, as well as cFSPTs without U(1) conservation, with U(1) but without TRS, or with a subset of all possible spatial symmetries has been reported [78–82, 88]. However, a complete classification of interacting cFSPT phases with the symmetries of class AII and all space groups is so-far missing. In this work, we take a step forward in filling this gap by classifying all cFSPT phases in two-dimensional (2D) space in class AII, enriched by any of the 17 wallpaper groups. Using the real-space construction scheme described in Refs. 78–82, for each wallpaper group we tabulate the total classification and its decomposition in terms of classification of lower-dimensional FSPTs. Incidentally, we realize that Wyckoff positions [89] of a given wallpaper group provide a natural guideline for possible decorations, therefore bridging a well-known notion in the context of crystalline lattices with the concept of ‘unit-cell subdivision’ adopted in Refs. 78–82. Interestingly, we find that all appropriate and nontrivial one-dimensional (1D) decorations at mirror symmetric lines correspond to intrinsically interacting cFSPT phases protected by the mirror symmetry. We provide toy-model Hamiltonians for both zero-dimensional (0D) and 1D decorations.

The rest of the paper is organized as follows. In Sec. II, we review the classification scheme we adopted, and we explicitly study the case of the honeycomb lattice, i.e., wallpaper group No. 17 ( $p6mm$ ) [89]. Therein, the classification for all wallpaper groups, our main result, is summarized in Table I. Section III presents toy model Hamiltonians that can be used to decorate the points and lines of the 2D lattice. Section IV discusses various signatures of cFSPT phases. Finally in Sec. V we draw the conclusion and provide an outlook. Appendixes A and B provide details on the classification of lower-dimensional decorations.

#	Wallpaper group	Classification
1	$p1$	$\mathbb{Z} \times \mathbb{Z}_2$
2	$p2$	$\mathbb{Z} \times (\mathbb{Z}_2)^4 \times (\mathbb{Z}_2)^4 \times \mathbb{Z}_2$
3	$p1m1$	$\mathbb{Z} \times (\mathbb{Z}_2)^2 \times (\mathbb{Z}_2)^4 \times \mathbb{Z}_2$
4	$p1g1$	$\mathbb{Z} \times \mathbb{Z}_2$
5	$c1m1$	$\mathbb{Z} \times \mathbb{Z}_2 \times (\mathbb{Z}_2)^2 \times \mathbb{Z}_2$
6	$p2mm$	$\mathbb{Z} \times (\mathbb{Z}_2)^4 \times (\mathbb{Z}_2)^{12} \times \mathbb{Z}_2$
7	$p2mg$	$\mathbb{Z} \times (\mathbb{Z}_2)^3 \times (\mathbb{Z}_2)^4 \times \mathbb{Z}_2$
8	$p2gg$	$\mathbb{Z} \times (\mathbb{Z}_2)^2 \times (\mathbb{Z}_2)^2 \times \mathbb{Z}_2$
9	$c2mm$	$\mathbb{Z} \times (\mathbb{Z}_2)^3 \times (\mathbb{Z}_2)^7 \times \mathbb{Z}_2$
10	$p4$	$\mathbb{Z} \times (\mathbb{Z}_4)^2 \times \mathbb{Z}_2 \times (\mathbb{Z}_2)^3 \times \mathbb{Z}_2$
11	$p4mm$	$\mathbb{Z} \times (\mathbb{Z}_4)^2 \times \mathbb{Z}_2 \times (\mathbb{Z}_2)^9 \times \mathbb{Z}_2$
12	$p4gm$	$\mathbb{Z} \times (\mathbb{Z}_4)^2 \times \mathbb{Z}_2 \times (\mathbb{Z}_2)^4 \times \mathbb{Z}_2$
13	$p3$	$\mathbb{Z} \times (\mathbb{Z}_3)^3 \times \mathbb{Z}_2$
14	$p3m1$	$\mathbb{Z} \times (\mathbb{Z}_3)^3 \times (\mathbb{Z}_2)^2 \times \mathbb{Z}_2$
15	$p31m$	$\mathbb{Z} \times (\mathbb{Z}_3)^2 \times (\mathbb{Z}_2)^2 \times \mathbb{Z}_2$
16	$p6$	$\mathbb{Z} \times \mathbb{Z}_6 \times \mathbb{Z}_3 \times \mathbb{Z}_2 \times (\mathbb{Z}_2)^2 \times \mathbb{Z}_2$
17	$p6mm$	$\mathbb{Z} \times \mathbb{Z}_6 \times \mathbb{Z}_3 \times \mathbb{Z}_2 \times (\mathbb{Z}_2)^6 \times \mathbb{Z}_2$

TABLE I. Classification of class AII cFSPTs for each of the 17 wallpaper groups. Each wallpaper group classification contains a  $\mathbb{Z}$  factor corresponding to the total number of Kramers’ pairs in the unit-cell, and a  $\mathbb{Z}_2$  factor for the intrinsic 2D SPT phase (the 2D “topological insulator”). The latter is colored in magenta to differentiate this phase which does not require crystalline symmetries nor interactions to be realized. The interaction enabled entries are highlighted in cyan, while the remaining entries are left in black.

## II. CLASSIFICATION BY REAL-SPACE CONSTRUCTION

Following Refs. 78–82, we are going to construct 2D cFSPT phases by decorating high-symmetry points, lines, and planes in space with appropriate FSPT phases, which are protected by internal symmetries only. The key idea behind this construction is that crystalline symmetries act as internal symmetries on those lower-dimensional subspaces that are invariant under their action.

In Sec. II A, we give an overview of the real-space construction of cFSPT phases in 2D. In Sec. II B, we specialize to the case of class AII and discuss which internal symmetries can arise at lower-dimensional subspaces. Therein, we provide a classification of lower-dimensional FSPT phases protected by these symmetries, and we define topological indices that distinguish possible decorations. In Sec. II D, we apply our scheme to classify cFSPT phases in class AII on a hexagonal lattice which has the wallpaper group  $p6mm$ .

Our main result is summarized by Table I, which lists the cFSPT classification in class AII for each of the 17 wallpaper groups. Many of the phases listed in the classification are intrinsically interacting (cyan entries), meaning that they can not be realized in the absence of interactions.

## A. Overview of real-space construction

For a given wallpaper group, we construct cFSPTs by following the construction based on “decorating” subspaces of the 2D space, which has been applied for classifying bosonic SPTs protected by point group symmetry, and cFSPTs in classes A and D of the 10-fold way enriched by various crystalline symmetries [78–82, 88, 90]. In the following, we summarize the steps for the cFSPT construction through decoration, adapted to our case of class AII.

1. *Unit-cell subdivision.* First, we divide the 2D space into unit-cells, which is allowed by the translation symmetries of the underlying lattice structure. We then subdivide each unit-cell into  $d$ -dimensional subspaces, where  $d = 0, 1, 2$ , which are invariant under some, or none, for the case of  $d = 2$ , of the crystalline symmetries. Our construction differs from the previous work in Refs. 78–82, and 90 by how we subdivide the unit-cells. We obtain the relevant subspaces by considering the coordinates of the Wyckoff positions of the lattice (see Sec. II C, for a review of Wyckoff positions and their relevant properties). If a given Wyckoff position has  $d$  free parameters in its coordinate definition, we consider  $d$ -dimensional finite subspaces in the unit-cell spanned by varying the free parameters of the coordinates. We refer to such subspaces as  $d$ -dimensional *Wyckoff patches*, where  $d$  is equal to the number of free parameters in the definition of the Wyckoff position’s coordinates. This defines our  $d$ -dimensional subspaces, to be decorated by FSPT phases.

2. *Decorating Wyckoff patches by FSPTs.* A given  $d$ -dimensional Wyckoff patch may be left invariant under some of the crystalline symmetries such as rotations or reflections, which act internally within the Wyckoff patch. For each such  $d$ -dimensional Wyckoff patch, we enumerate all the possible  $d'$ -dimensional FSPTs ( $d' \leq d$ ) that can be “glued” to that patch, which we call *decorations*. The possible decorations are then  $d'$ -dimensional FSPT phases protected by the internal symmetries of class AII, together with the crystalline symmetries that leave the corresponding Wyckoff patch invariant. We enumerate distinct decorations by assigning a topological index to each decoration. These indicate how the protecting symmetries are represented at a given Wyckoff patch. In Sec. II B, we detail the classification of possible  $d'$ -dimensional FSPT decorations. We remark that decorating a Wyckoff position with an FSPT does not imply that a physical degree of freedom (atom) needs to be placed there [see e.g., Fig. 3(c)].

3. *Choosing gappable decorations.* Since cFSPT phases are gapped in the bulk by definition, we must consider only decorations that can be gapped out in the bulk while preserving the crystalline symmetries. We call such decorations *gappable*, and otherwise they are *non-gappable*. By definition, all 0D decorations are already gapped. Therefore, the only potentially non-gappable decorations are either 1D or 2D. Let us first consider the

case of 1D decorations. If there exist any nontrivial 1D FSPT protected by the symmetries of a specific line in the 2D bulk, we can glue such 1D phases along such a line. Each glued 1D FSPT supports 0D gapless boundary modes. To ensure that this construction results into a gappable phase, multiple of these 1D FSPTs must meet at their endpoints in an appropriate number and arrangement, such that their gapless boundary modes can be gapped out by interactions that are compatible with all the protecting symmetries. Likewise, for nontrivial 2D decorations we have to ensure that gapless 1D boundary modes are gapped out in the bulk without breaking any crystalline symmetry.

4. *Equivalences.* The last step is to identify equivalences between distinct decorations of lower-dimensional FSPT phases. Two decorations are equivalent if they can be connected by symmetric and gap preserving local processes. As we shall demonstrate in Sec. II D for wallpaper group  $p6mm$ , these equivalences take the form of moving 0D FSPT decorations from one Wyckoff position to another. The cFSPT classification is then given by enumerating gappable decorations modulo equivalences under adiabatic deformations.

In practice, the classification is a collection of topological indices labeling all the inequivalent topological phases realized by various decorations. At the same time, this approach gives a prescription to construct many-body wave functions that realize the phase corresponding to a chosen set of topological indices as product states of decorations.

## B. Classification of possible decorations

The symmetry class AII refers to the FSPT phases with charge-conservation and spinful TRS symmetries. More precisely, we denote the symmetry group by

$$G_f^{\text{AII}} := \frac{U(1)^F \rtimes \mathbb{Z}_4^{\text{FT}}}{\mathbb{Z}_2^F}, \quad (1)$$

which comprises two subgroups. First, the subgroup  $U(1)^F$  corresponds to the charge-conservation symmetry. The superscript F is to indicate that this subgroup contains the fermion parity symmetry  $\mathbb{Z}_2^F$ .<sup>2</sup> Second, the subgroup  $\mathbb{Z}_4^{\text{FT}}$  corresponds to the spinful TRS. Here too the superscript indicates that this subgroup contains fermion parity symmetry, since for spinful fermions TRS squares to fermion parity. To avoid double counting the fermion parity symmetry, we coset by the subgroup  $\mathbb{Z}_2^F$ .

As described in Sec. II A, we should classify FSPT phases in  $d' = 0, 1, 2$  dimensions that are protected by

<sup>2</sup> If we parameterize the elements of  $U(1)^F$  by  $e^{i\theta}$  with  $\theta \in [0, 2\pi)$ , then fermion parity symmetry is generated by the element  $\theta = \pi$ . Fermion parity is a symmetry of any Hamiltonian built out of fermions and cannot be broken explicitly or spontaneously.

$d'$	CS	cFSPT Classification
0D	$\mathbb{Z}_{2a}^F \rtimes \mathbb{Z}_{2b}^F / \mathbb{Z}_2^F$	$\mathbb{Z} \times \mathbb{Z}_{\gcd(2,a)} \times \mathbb{Z}_b$
1D	$\mathbb{Z}_{2b}^F$	$\mathbb{Z}_b$
2D	$\mathbb{Z}_1$	$\mathbb{Z}_2$

TABLE II. Classification of FSPTs in  $d' = 0, 1, 2$  with full symmetry group  $G_{f,\text{tot}}^{(d')}$ , obtained by appropriately combining the group in Eq. (1) with the group of crystalline symmetries acting internally, which is listed under the column CS. The total symmetry group  $G_{f,\text{tot}}^{(d')}$  obtained this way is explicitly shown in Eqs. (2), (4), and (6) for  $d' = 0, 1, 2$ , respectively. The third column, labeled cFSPT Classification, contains the resulting classification as obtained from cohomology groups. The color code follows the one of Tab. I.

the symmetries of class AII together with any crystalline symmetries that act internally on subspaces of the 2D space. In Table II, we summarize the classification of all possible FSPT decorations in  $(d' = 0, 1, 2)$ -dimensional subspaces. In what follows, we explain how this table is obtained by enumerating possible enhancements of the symmetry group  $G_f^{\text{AII}}$  by crystalline symmetries, and we classify the corresponding FSPT phases.

1. *Classification of 0D decorations.* A subspace in  $d' = 0$  dimension can be kept invariant under the action of point group symmetries. In 2D, there are ten possible double point groups, all of the form  $(\mathbb{Z}_{2a}^F \rtimes \mathbb{Z}_{2b}^F) / \mathbb{Z}_2^F$ , where  $a = 1, 2, 3, 4, 6$  denotes the  $a$ -fold rotation while  $b = 1, 2$  denotes the absence ( $b = 1$ ) or presence ( $b = 2$ ) of a mirror symmetry. Since we consider spinful fermions, both  $2\pi$  rotations and applying mirror transformation twice must be equal to fermion parity symmetry. In other words, at a 0D subspace the total symmetry group  $G_{f,\text{tot}}^{(0)}$  is

$$G_{f,\text{tot}}^{(0)} := G_f^{\text{AII}} \times \frac{\mathbb{Z}_{2a}^F \rtimes \mathbb{Z}_{2b}^F}{\mathbb{Z}_2^F \times \mathbb{Z}_2^F}, \quad (2)$$

for  $a = 1, 2, 3, 4, 6$  and  $b = 1, 2$ . In 0D, the FSPT phases protected by  $G_{f,\text{tot}}^{(0)}$  are classified by the first cohomology group [61, 65]

$$H^1(G_{f,\text{tot}}^{(0)}, U(1)) = \mathbb{Z} \times \mathbb{Z}_{\gcd(2,a)} \times \mathbb{Z}_b, \quad (3)$$

where  $\gcd(2, a)$  is the greatest common divisor of integers  $a$  and 2. The first cohomology group  $H^1$  classifies the 1D representations of the total symmetry group (2), i.e., possible charges of a 0D quantum state  $|\Psi\rangle$  that are compatible with the group composition rule. Such a state  $|\Psi\rangle$  is precisely the 0D decoration one can attach to a high-symmetry point that is invariant under the  $(\mathbb{Z}_{2a}^F \rtimes \mathbb{Z}_{2b}^F) / \mathbb{Z}_2^F$  double point group symmetry.

The  $\mathbb{Z}$  term in Eq. (3) is the classification of 0D FSPT phases protected only by charge-conservation and spinful TRS. Physically, it corresponds to the total number of Kramers' pairs localized at the high-symmetry point,

which we denote by the index  $n \in \mathbb{Z}$ . The remaining two terms  $\mathbb{Z}_{\gcd(2,a)} \times \mathbb{Z}_b$  give the classification of 0D FSPT phases protected by the point group symmetries. Because of TRS, any 0D decoration can only carry real charges, i.e.,  $\pm 1$ , under rotation and mirror symmetries. Whenever  $\gcd(2, a) = 2$  or  $b = 2$ , we define two  $\mathbb{Z}_2$ -valued indices  $r \in \mathbb{Z}_2$  and  $m \in \mathbb{Z}_2$ , which label the rotation and mirror charges, respectively, of a 0D decoration. Crucially, these  $\mathbb{Z}_2$  indices are absent in noninteracting electronic systems in AII, where wave functions can only transform trivially under the action of rotations or mirror transformations [91]. As we shall discuss in Sec. III, all 0D decorations with nontrivial indices  $r$  or  $m$  are intrinsically interacting.

2. *Classification of 1D decorations.* For 1D decorations in 2D space, only mirror transformation can act internally. Therefore, the total symmetry group becomes

$$G_{f,\text{tot}}^{(1)} := G_f^{\text{AII}} \times \frac{\mathbb{Z}_{2b}^F}{\mathbb{Z}_2^F}, \quad (4)$$

where  $b = 1$  or  $b = 2$  denotes the absence or presence of mirror symmetry, respectively. In 1D, the FSPT phases protected by  $G_{f,\text{tot}}^{(1)}$  are classified by the second cohomology group [92–94]

$$H^2(G_{f,\text{tot}}^{(1)}, U(1)) = \mathbb{Z}_b. \quad (5)$$

It classifies the projective representations of the total symmetry group (4). There are no nontrivial FSPT phases protected only by charge-conservation and spinful TRS symmetries. Therefore, the classification (5) corresponds to the 1D FSPT decorations that are stabilized by the presence of the mirror symmetry. Physically, a nontrivial 1D decoration features gapless Kramers' pairs at its 0D boundaries, protected by the total symmetry group in Eq. (4). The  $\mathbb{Z}_b$  group in Eq. (5) then corresponds to the parity of the number of Kramers' pairs at the boundary, which we denote by the index  $\nu \in \mathbb{Z}_2$ . We dub the phase realized by nontrivial 1D decorations the *AIIM phase*, since it is protected by the symmetries of class AII and mirror symmetry, and we refer to  $\nu$  as the AIIM index. In Sec. III, we demonstrate that the AIIM phase is intrinsically interacting and we introduce a model Hamiltonian realizing it.

3. *Classification of 2D decorations.* There are no crystalline symmetries in 2D space that leave a 2D decoration invariant. Therefore, the total symmetry group for  $(d' = 2)$ -dimensional decorations is simply

$$G_{f,\text{tot}}^{(2)} := G_f^{\text{AII}}. \quad (6)$$

In 2D, FSPT phases protected by  $G_f^{\text{AII}}$  symmetry are  $\mathbb{Z}_2$  classified [6, 66, 68]. The nontrivial 2D FSPT phase in class AII features gapless helical boundary states, and it is such that odd number of boundary states cannot be gapped unless TRS is broken. We define the index  $x \in \mathbb{Z}_2$  that labels if a 2D decoration is trivial or not, and physically corresponds to the parity of the number of helical edge states.



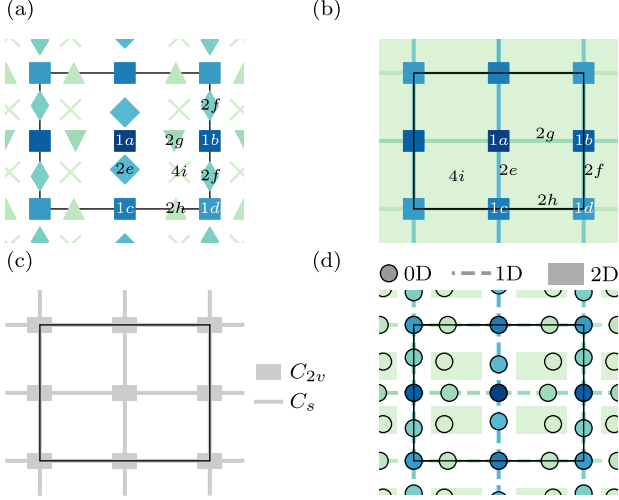


FIG. 1. (a) Wyckoff positions of the wallpaper group  $p2mm$  (No. 6) with their labels and (c) illustration of the nontrivial site-symmetry groups of the lattice [either  $C_{2v}$  or  $C_s$  (marked in gray)]. (b) Unit cell subdivision based on Wyckoff patches: 0D (circles), 1D (lines), and 2D (rectangles) patches are colored and labeled according to their corresponding Wyckoff position, following the color code of (a). (d) Example of 0D (dots), 1D (dashed lines), or 2D (rectangular regions) FSPTs decorations of the  $p2mm$  lattice. Decorations are colored according to the Wyckoff position to which they belong, following the color code in (a). In all panels, a unit-cell is marked by black lines.

### C. Decorating Wyckoff patches

We start this section by briefly recalling some useful concepts in the description of crystalline lattices. Every point in the lattice is characterized by its site-symmetry group, namely the finite subgroup of the space group transformations that leave the point invariant. A Wyckoff position is a set of points in the lattice whose site-symmetry groups are conjugate subgroups of the space group, i.e., the two site-symmetry groups are related by an element of the space group. Wyckoff positions are labeled by their multiplicity followed by a letter, and they are tabulated for all the space groups [89]. The “generic position” on a 2D lattice is the Wyckoff position with trivial site-symmetry group. The coordinates of the Wyckoff positions can either be fully determined or defined up to some free parameters.

1. *Wyckoff patches.* We now introduce the concept of *Wyckoff patches*: Given a Wyckoff position with  $d$  free parameters in the definition of its coordinates, we call the  $d$ -dimensional region of the unit-cell covered by varying the free parameters a  $d$ -dimensional Wyckoff patch.

By extension, we call the *site-symmetry group of the Wyckoff patch* the site-symmetry group of the Wyckoff position spanning the patch. Wyckoff positions with nontrivial site-symmetry groups lead to either 0D or 1D

$d$	SG	Wyckoff patch classification
0D	$C_k$	$\mathbb{Z} \times \mathbb{Z}_{\text{gcd}(k,2)}$
	$C_{kv}$	$\mathbb{Z} \times \mathbb{Z}_{\text{gcd}(k,2)} \times \mathbb{Z}_2$
1D	$C_s$	$\mathbb{Z} \times \mathbb{Z}_2 \times \mathbb{Z}_2$
2D	$C_1$	$\mathbb{Z} \times \mathbb{Z}_2$

TABLE III. Classification of decorations on  $d$ -dimensional Wyckoff patches. The SG column distinguishes the site-symmetry group of the Wyckoff position, and the last column shows the full classification. The color code follows the one introduced in Tab. I.

patches, while the general position results into a 2D patch. As Wyckoff positions provide a natural way to systematically characterize the lattice, we employ the concept of  $d$ -dimensional Wyckoff patches as our definition of unit-cell subdivision.

As an example, Fig. 1(a) illustrates the Wyckoff positions of the unit-cell of the wallpaper group No. 6 ( $p2mm$ ) and Fig. 1(c) the corresponding site-symmetry group at each point. For instance, the explicit coordinates of the Wyckoff positions  $1a$ ,  $2e$  and  $4i$  are

$$\begin{aligned}
 1a &: (0, 0), \\
 2e &: (x, 0), (-x, 0) \\
 4i &: (x, y), (-x, y), (x, -y), (-x, -y)
 \end{aligned} \tag{7}$$

where we expressed coordinates in terms of lattice vectors, namely  $(x, y) = x\mathbf{a}_x + y\mathbf{a}_y$  with  $\mathbf{a}_x = a\hat{x}$ ,  $\mathbf{a}_y = b\hat{y}$  ( $a \neq b$ ), and the parameters  $x, y$  are undetermined. From Eq. (7), we deduce that the  $1a$ ,  $2e$ , and  $4i$  Wyckoff positions result into 0D, 1D, and 2D Wyckoff patches, respectively. The  $4i$  Wyckoff position is the general position of the lattice, it has trivial site-symmetry group and its coordinates span the full 2D space. From the Wyckoff patches, we identify the subdivision of the unit-cell of  $p2mm$ , as shown in Fig. 1(b).

2. *Decorations.* With our newly introduced notion of unit-cell subdivision, we can proceed and answer the question of how to decorate unit-cells. A  $d$ -dimensional Wyckoff patch can be decorated by cFSPTs that: (i) are  $d'$ -dimensional, with  $d' \leq d$ , and (ii) are protected by the site-symmetry group of the Wyckoff patch and class AII.

The site-symmetry groups of Wyckoff patches are drawn from the same set of crystalline symmetries considered in Sec. II B, and they are as follows: 0D Wyckoff patches have  $\mathbb{Z}_{2a}^F \times \mathbb{Z}_{2b}^F$  ( $a = 2, 3, 4, 6$ ,  $b = 1, 2$ ) symmetry, 1D have  $\mathbb{Z}_{2b}^F$  mirror symmetry, and 2D do not have additional symmetries hence the onsite group is  $\mathbb{Z}_1$ .

By appropriately combining the entries of Table II, we can deduce the classification of the possible decorations on Wyckoff patches fulfilling (i) and (ii). The resulting classification is summarized in Table III. The 0D Wyckoff patches can only be decorated by 0D cFSPTs, therefore the 0D entry of Tab. II exhausts their classification. The 1D Wyckoff patches can either be deco-

$d$	Wyckoff position	SG	Classification	indices
0D	1a	$C_{6v}$	$\mathbb{Z} \times \mathbb{Z}_2 \times \mathbb{Z}_2$	$n_{1a}, r_{1a}, m_{1a}$
	2b	$C_{3v}$	$\mathbb{Z} \times \mathbb{Z}_2$	$n_{2b}, m_{2b}$
	3c	$C_{2v}$	$\mathbb{Z} \times \mathbb{Z}_2 \times \mathbb{Z}_2$	$n_{3c}, r_{3c}, m_{3c}$
1D	6d	$C_s$	$\mathbb{Z} \times \mathbb{Z}_2 \times \mathbb{Z}_2$	$n_{6d}, m_{6d}, \nu_{6d}$
	6e	$C_s$	$\mathbb{Z} \times \mathbb{Z}_2 \times \mathbb{Z}_2$	$n_{6e}, m_{6e}, \nu_{6e}$
2D	12f	$C_1$	$\mathbb{Z} \times \mathbb{Z}_2$	$n_{12f}, x_{12f}$

TABLE IV. Decorations for the wallpaper group  $p6mm$  (No. 17). The  $d$ , Wyckoff position, and SG columns list the dimension, label, and site-symmetry group for the Wyckoff positions of  $p6mm$ . The classification of the decorations and their indices are listed in the last two columns.

rated by 1D cFSPTs, resulting into a  $\mathbb{Z}_2$  contribution to the classification, or by 0D cFSPTs, leading to an additional  $\mathbb{Z} \times \mathbb{Z}_2$  factor corresponding to the total number of Kramers' pairs and total mirror eigenvalue of the 0D decorations, respectively. In fact, when multiple 0D decorations are stacked on a 1D line, they can be symmetrically and adiabatically moved along the line, and therefore the only relevant set of topological indices is the one counting their total charges per unit-cell. The 2D Wyckoff patches do not have any crystalline symmetry acting internally, therefore the contribution of 2D decorations is given by the  $\mathbb{Z}_2$  graded 2D AII classification. Decorating these Wyckoff patches by 1D cFSPTs does not enrich the classification, as these must be trivial in the absence of additional internal symmetries, while 0D decorations contribute a  $\mathbb{Z}$  index enumerating the total number of Kramers' pairs. We label decorations at a Wyckoff patch by the topological indices introduced in Sec. II B with a subscript denoting the corresponding Wyckoff position. For instance, in the unit-cell subdivision shown in Fig. 1, 0D FSPTs that can be glued to the 0D Wyckoff patch 1a are characterized by the triplet  $n_{1a}$ ,  $r_{1a}$ , and  $m_{1a}$  that indicate the total number of Kramers' pairs, their charge under rotations, and their charge under mirror symmetry, respectively. Figure 1(d) shows a possible set of decorations on the  $p2mm$  lattice.

#### D. Example: Wallpaper group No. 17

Let us now discuss as an explicit example the case of wallpaper group  $p6mm$  (No. 17) [Fig. 2(a), (b)].

To find the classification of  $p6mm$ , we follow the procedure outlined in Sec. II: (i) we subdivide the unit-cell into Wyckoff patches, (ii) we enumerate the decorations for all the Wyckoff patches, (iii) we then identify the gappable decorations, (iv) and we identify equivalent decorations.

1. *Unit cell subdivision.* The unit-cell subdivision is done based on the notion of Wyckoff patches. The Wyckoff positions and the site-symmetry group of the points in the unit-cell are shown in Fig. 2(a),(b) and are listed

in Table IV. The unit-cell of this space group contains three 0D Wyckoff patches, 1a, 2b, and 3c, two 1D Wyckoff patches, 6d and 6e, and the 2D Wyckoff patch 12f.

2. *Enumeration of decorations.* The set of possible decorations of the  $p6mm$  lattice alongside the indices that classify the decorations are summarized in Table IV and depicted in Figs. 2(c)–(f). For the 0D Wyckoff patches, the indices describing the decorations are the total number of Kramers' pairs at each Wyckoff patch

$$(n_{1a}, n_{2b}, n_{3c}) \in (\mathbb{Z})^3 \quad (8)$$

and the rotation and mirror charges

$$(r_{1a}, m_{1a}, m_{2b}, r_{3c}, m_{3c}) \in (\mathbb{Z}_2)^5. \quad (9)$$

The 1D Wyckoff patches are endowed with the AIIM indices

$$(\nu_{6d}, \nu_{6e}) \in (\mathbb{Z}_2)^2, \quad (10)$$

and the number of Kramers' pairs and mirror charges stemming from 0D decorations

$$(n_{6d}, n_{6e}, m_{6d}, m_{6e}) \in (\mathbb{Z})^2 \times (\mathbb{Z}_2)^2. \quad (11)$$

Finally, 2D patches are classified by the number of Kramers' pairs of 0D decorations and the 2D AII topological phase index

$$(n_{12f}, x_{12f}) \in \mathbb{Z} \times \mathbb{Z}_2. \quad (12)$$

3. *Gappable decorations.* We now rule out those decorations that result in gapless modes appearing in the bulk, and we consider 0D, 1D and 2D decorations one by one. All the 0D decorations are gappable, therefore there is no reduction of any of the indices counting the Kramers' pairs or mirror and rotation charges due to the requirement of gappability [Fig. 2(c)]. For 1D decorations on the 6e Wyckoff patches, there is only one minimal way to decorate the unit-cells such that six lines meet at every crossing point, allowing to gap the edge modes in the bulk, while other decorations are not gappable: If we choose the 6e patches to terminate at the 2b patch, whose site-symmetry group contains mirror and three-fold rotation symmetries, there would be three 0D gapless boundary modes meeting at a point that are not gappable, and such a decoration has to be discarded [Fig. 2(e)]. However, if the 6d patches are continued to the next 1a position, the resulting decoration is gappable [Fig. 2(f)]. The 1D decorations along the 6d patches are symmetry constrained to meet in even number at every crossing point, therefore, they can be gapped out in the bulk [Fig. 2(f)]. Likewise, the edge modes on neighboring 2D Wyckoff patches can be gapped out by covering the whole 2D space by the same phase [Fig. 2(d)].

4. *Equivalences.* We now consider the equivalences that reduce the set of indices listed above by connecting different phases through adiabatic and symmetric transformations. We start by listing the processes of peeling off charges: For example,  $6k$  Kramers' pairs can be

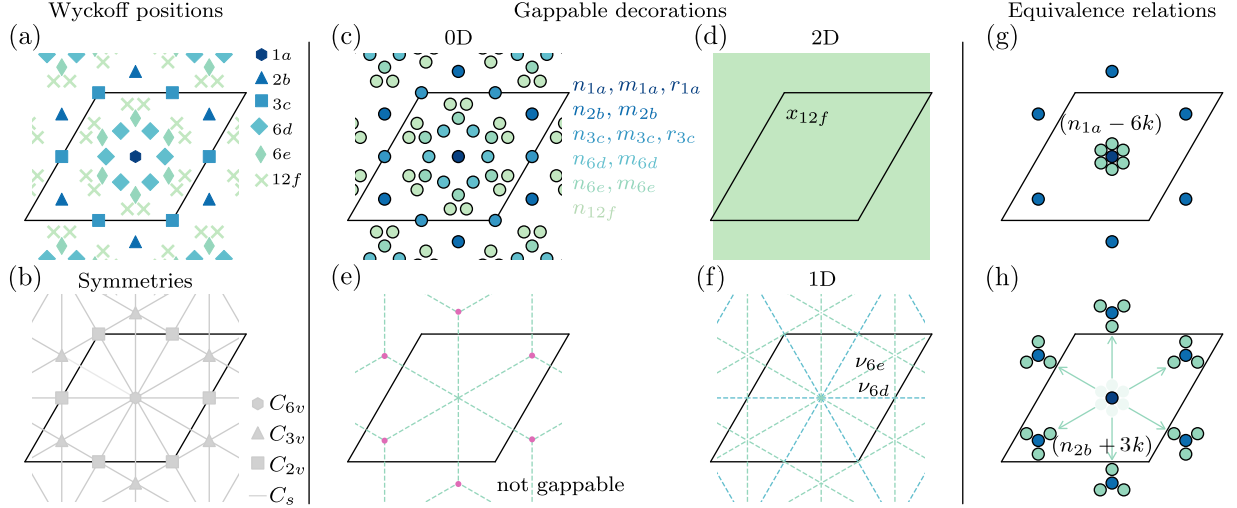


FIG. 2. (a) Wyckoff positions of the wallpaper group  $p6mm$  (No. 17) and (b) mirror axes and rotation centers of the unit-cell, corresponding to the nontrivial site-symmetry groups in the unit-cell. (c)–(f) Representation of (c) 0D, (e), (f) 1D, and (d) 2D gappable decorations of Wyckoff patches, with the corresponding indices listed. In (e), we show an example of non-gappable decoration, and therefore with no index associated to it. (g), (h) Exemplification of the equivalence process  $n_{1a}, n_{2b} \rightarrow n_{1a} - 6k, n_{2b} + 3k$ , described around Eq. (13) in the main text.

pulled away from the  $1a$  Wyckoff patch, moved along the  $6e$  lines, and brought to the  $2b$  Wyckoff patches. This is illustrated in Figs. 2(g) and 2(h). We write this process as

$$(n_{1a}, n_{2b}) \rightarrow (n_{1a} - 6k, n_{2b} + 3k), \quad (13)$$

while all the remaining indices are left unchanged. Similarly, the following processes are allowed

$$\begin{aligned} (n_{1a}, n_{3c}) &\rightarrow (n_{1a} - 6k, n_{3c} + 2k), \\ (n_{1a}, n_{6d}) &\rightarrow (n_{1a} - 6k, n_{6d} + k), \\ (n_{1a}, n_{6e}) &\rightarrow (n_{1a} - 6k, n_{6e} + k), \\ (n_{1a}, n_{12f}) &\rightarrow (n_{1a} - 12k, n_{12f} + k). \end{aligned} \quad (14)$$

From the collection of equivalences listed above, we identify the following independent indices:

$$\begin{aligned} (n_{1a}, n_{2b}, n_{3c}, n_{6e}, n_{6d}, n_{12f}) &\in (\mathbb{Z})^6 \\ \rightarrow (n_{1a}, n_{2b}, n_{3c}) &\in \mathbb{Z}_6 \times \mathbb{Z}_3 \times \mathbb{Z}_2, \end{aligned} \quad (15)$$

and bearing in mind that there is still a well defined index counting the total number of Kramers' pair in the unit-cell,  $n \in \mathbb{Z}$ . Another set of reduction is realized by the neutralization of the mirror charges where an odd number of Wyckoff patches meet. In particular, the  $m_{2b}$  and  $m_{6e}$  indices reduce to trivial and therefore are dropped out in the classification (Appendix A).

The overall classification of  $p6mm$  cFSPTs finally becomes

$$\mathbb{Z} \times \mathbb{Z}_6 \times \mathbb{Z}_3 \times (\mathbb{Z}_2)^6 \times \mathbb{Z}_2. \quad (16)$$

In this classification, the  $(\mathbb{Z}_2)^6$  contribution, with indices  $(r_{1a}, m_{1a}, r_{3c}, m_{3c}, \nu_{6d}, \nu_{6e}) \in (\mathbb{Z}_2)^6$ , is both intrinsically interacting and requires crystalline symmetries to

exist. For this reason, they are highlighted in cyan in Table I.

All the remaining wallpaper groups are treated similarly, and the resulting classification is contained in Table I, where entries corresponding to intrinsically interacting phases are highlighted. The key steps followed towards filling Table I are reported in Appendix B, where we also list the decoration indices corresponding to each wallpaper group classification explicitly.

### III. HAMILTONIAN REALIZATIONS

We present some of the possible Hamiltonian realizations for the 0D and 1D decorations. From the latter, one can construct toy Hamiltonians for the full 2D cFSPTs by taking the transitionally invariant sums of 0D and 1D Hamiltonians acting on the appropriate Wyckoff patches. We do not discuss the case of 2D Wyckoff patches, as there are no crystalline symmetries acting onsite, and the  $\mathbb{Z}_2$  classification that arises without crystalline symmetries. An example of realization of the nontrivial phase is for instance the Kane-Mele model, for the case of non-interacting fermions [95].

#### A. 0D FSPTs: Mott atomic limits

Noninteracting electronic gapped and non-degenerate ground states with TRS and particle conservation are constrained to transform trivially under the action of

crystalline symmetries [91]

$$\hat{U}(s) |\Psi_{\text{nonint}}\rangle = + |\Psi_{\text{nonint}}\rangle, \quad (17)$$

for any element  $s$  in the space group, provided that  $\hat{U}(s)$  is a symmetry of both the ground state and the Hamiltonian. However, Eq. (17) does not necessarily hold in interacting systems. Therefore, for indices  $r = \pm 1$  and  $m = \pm 1$  that label the rotation and mirror charge of 0D decorations can only be nontrivial in the presence of interactions.

An example of a 0D system where the interacting ground state transforms nontrivially under crystalline symmetries is the ‘Hubbard square’, a four-site square molecule with a spinful orbital located at each corner of the square [91, 96–98] [Fig. 3(a)]. The Hamiltonian is given by

$$\begin{aligned} \hat{H}_{\text{HS}} = & \sum_{i=1}^4 \sum_{\sigma=\uparrow,\downarrow} \left[ -t_1 (\hat{c}_{i,\sigma}^\dagger \hat{c}_{i+1,\sigma} + \text{H.c.}) + t_2 \hat{c}_{i,\sigma}^\dagger \hat{c}_{i+2,\sigma} \right] \\ & + U \sum_{i=1}^4 \hat{n}_{i,\uparrow} \hat{n}_{i,\downarrow} - \mu \sum_{i=1}^4 \sum_{\sigma} \hat{n}_{i,\sigma}, \end{aligned} \quad (18)$$

where  $\hat{c}_{i,\sigma}$  ( $\hat{c}_{i,\sigma}^\dagger$ ) denotes the annihilation (creation) operator of the electronic state at the  $i$ -th corner with spin  $\sigma \in \{\uparrow, \downarrow\}$ ,  $t_1$  and  $t_2$  are the tunneling amplitude along the square edges and diagonals, respectively,  $U$  is the Hubbard coupling, and  $\mu$  the chemical potential. In the  $C_4$  eigenbasis, the electronic operators are

$$\hat{c}_{\ell,\sigma} = \frac{1}{2} \sum_{i=1}^4 e^{i2\pi i\ell/4} \hat{c}_{i,\sigma}, \quad \ell = 0, \frac{\pi}{2}, \pi, -\frac{\pi}{2}. \quad (19)$$

At half-filling, for  $t_1 > t_2$  ( $t_1 < t_2$ ) and  $U > 0$ , the ground state of Eq. (18) transforms with  $-1$  ( $+1$ ) under the action of  $C_4$  rotation symmetry. Expressed in the basis (19), the ground state in the limit  $U \rightarrow 0$  and  $t_1 > t_2$  can be written as [91]

$$|\Psi_{\text{HS}}\rangle = \frac{1}{\sqrt{2}} \hat{c}_{0,\uparrow}^\dagger \hat{c}_{0,\downarrow}^\dagger (\hat{c}_{\frac{\pi}{2},\uparrow}^\dagger \hat{c}_{\frac{\pi}{2},\downarrow}^\dagger - \hat{c}_{-\frac{\pi}{2},\downarrow}^\dagger \hat{c}_{-\frac{\pi}{2},\uparrow}^\dagger) |0\rangle. \quad (20)$$

This ground state is symmetric under TRS and carries eigenvalue  $-1$  under the action of  $C_4$  rotation symmetry. Therefore, it realizes an example of 0D cFSPT with nontrivial rotation charge,  $r = -1$ . The state  $|\Psi_{\text{HS}}\rangle$  also carries nontrivial  $U(1)$ -charge since it is a linear combination of states with two Kramers’ pairs, i.e.,  $n = 2$ . To tune the indices  $n$  and  $r$  independently, we can construct another Hamiltonian  $\hat{H}'_{\text{HS}}$  that is related to  $\hat{H}_{\text{HS}}$  by the unitary particle hole symmetry  $\hat{c}_{i,\sigma}^\dagger \leftrightarrow \hat{c}_{i,\sigma}$ . Choosing ( $t_1 < t_2$ ) in Hamiltonian  $\hat{H}'_{\text{HS}}$  delivers a ground state  $|\phi_{\text{HS}}\rangle$  that carries  $n = -2$  and trivial rotation charge  $r = +1$ . Tensor product of the two ground states  $|\Psi_{\text{HS}}\rangle \otimes |\phi_{\text{HS}}\rangle$  is a 0D decoration with indices  $n = 0$  and  $r = 0$ .

Beyond the example of the Hubbard square, this construction can be extended to other point groups and used

to obtain cFSPTs as ground states of Hubbard Hamiltonians [99, 100]. The cFSPTs obtained as product states of 0D cFSPTs realized through Hubbard like Hamiltonians, so-called Mott atomic limits (MAL), were studied in Ref. 100. There, the cFSPT wave functions are written as

$$|\text{MAL}\rangle = \prod_{\mathbf{r} \in \Lambda} \hat{O}_{\mathbf{r}}^\dagger |0\rangle, \quad (21)$$

where each  $\hat{O}_{\mathbf{r}}^\dagger$  contains  $N$ -particle creation operators, and  $\hat{O}_{\mathbf{r}}^\dagger$ ’s commute at different sites, while they describe entangled states within the  $N$ -particles they create. Similar states are studied in Ref. 101.

## B. 1D FSPTs: The AIIM model

In Sec. IIB we have pointed out that fermionic 1D systems with TRS, particle-number conservation, and a mirror symmetry acting as an onsite symmetry have  $\mathbb{Z}_2$  classification. In this section, we propose a model Hamiltonian that realizes the nontrivial phase of this classification, which we dub the AIIM model.

To better understand this  $\mathbb{Z}_2$  classification, we notice that the internal symmetry group in Eq. (4) (with  $b = 2$ ) has the following isomorphism:

$$G_{f,\text{tot}}^{(1)} = \frac{G_f^{\text{AI}} \times \mathbb{Z}_4^{\text{F}}}{\mathbb{Z}_2^{\text{F}}} \cong G_f^{\text{AI}} \rtimes \mathbb{Z}_2^{T'}, \quad (22)$$

with  $\mathbb{Z}_2^{T'}$  being a spinless TRS whose generator is the product of the TRS and the mirror symmetry generators,  $t \in \mathbb{Z}_4^{\text{FT}}$  and  $m \in \mathbb{Z}_4^{\text{FM}}$ , i.e.,  $t' = tm$ . Indeed,  $t'$  is represented by an antiunitary operator which squares to the identity, and has a nontrivial action on the particle conservation  $U(1)^{\text{F}}$  subgroup. We claim that the 1D nontrivial FSPT phase with symmetry group (22) must be intrinsically interacting, meaning that there is no non-interacting counterpart of such a phase. The reason for this is as follows. The only nontrivial projective representation of group  $G_{f,\text{tot}}^{(1)}$  is when the representation  $\hat{U}(t')$  of element  $t'$  squares to minus identity. In other words, the nontrivial 1D FSPT with  $G_{f,\text{tot}}^{(1)}$  symmetry must support gapless boundary modes that realize a projective representation of the subgroup

$$U(1)^{\text{F}} \rtimes \mathbb{Z}_2^{T'} \subset G_{f,\text{tot}}^{(1)}, \quad (23)$$

which describes the symmetry class AI of the 10-fold way. It is known that the noninteracting classification for class AI in 1D is trivial [1–3], while its fully interacting classification is  $\mathbb{Z}_2$  [6].

We consider a 1D lattice of size  $L$  with each site  $j$  supporting two orbitals of spinful electrons [Fig. 3(b)]. The corresponding creation and annihilation operators satisfy

$$\{\hat{c}_{j,\alpha,\sigma}, \hat{c}_{j',\alpha',\sigma'}^\dagger\} = \delta_{j,j'} \delta_{\alpha,\alpha'} \delta_{\sigma,\sigma'}, \quad (24)$$



with orbital and spin indices  $\alpha = 1, 2$  and  $\sigma = \uparrow, \downarrow$ , respectively. To realize the intrinsically interacting 1D FSPT phase, we then propose the Hamiltonian

$$\begin{aligned} \hat{H}_{\text{AIIM}} = & - \sum_{j=1}^L \hat{Z}_j^f \hat{X}_{j+1}^f \hat{Z}_{j+2}^f \\ & + V \sum_{j=1}^L (\hat{n}_{j,1} - 1)(\hat{n}_{j,2} - 1), \end{aligned} \quad (25a)$$

where

$$\hat{n}_{j,\alpha} = \sum_{\sigma} \hat{n}_{j,\alpha,\sigma}, \quad \hat{n}_{j,\alpha,\sigma} = \hat{c}_{j,\alpha,\sigma}^\dagger \hat{c}_{j,\alpha,\sigma} \quad (25b)$$

are number operators, and  $\hat{Z}_j^f$  and  $\hat{X}_j^f$  are defined as

$$\begin{aligned} \hat{Z}_j^f &:= \frac{1}{2} \sum_{\alpha,\sigma} (-1)^{\alpha+1} \hat{n}_{j,\sigma,\alpha}, \\ \hat{X}_j^f &:= \hat{c}_{j,\uparrow,1}^\dagger \hat{c}_{j,\downarrow,1}^\dagger \hat{c}_{j,\downarrow,2} \hat{c}_{j,\uparrow,2} + \hat{c}_{j,\uparrow,2}^\dagger \hat{c}_{j,\downarrow,2}^\dagger \hat{c}_{j,\downarrow,1} \hat{c}_{j,\uparrow,1}. \end{aligned} \quad (25c)$$

In the AIIM Hamiltonian of Eq. (25), the first term contains four-body interactions while the second term is an onsite repulsive ( $V > 0$ ) interaction term. This Hamiltonian is symmetric under the action of the operators

$$\hat{U}(\theta) := e^{i\theta \sum_{j,\alpha,\sigma} \hat{n}_{j,\alpha,\sigma}}, \quad (26a)$$

$$\hat{U}(t) := e^{i\frac{\pi}{2} \sum_{j,\alpha} \sum_{\sigma,\nu} \hat{c}_{j,\alpha,\sigma}^\dagger \sigma_{\sigma,\nu}^y \hat{c}_{j,\alpha,\nu}} \mathbf{K}, \quad (26b)$$

$$\hat{U}(m) := e^{i\frac{\pi}{2} \sum_j \sum_{\alpha,\rho} \sum_{\sigma,\nu} \hat{c}_{j,\alpha,\sigma}^\dagger \tau_{\alpha,\rho}^x \sigma_{\sigma,\nu}^x \hat{c}_{j,\rho,\nu}}, \quad (26c)$$

that respectively implement  $U(1)$ , TRS, and the mirror transformations

$$\hat{U}(\theta) : \hat{c}_{j,\alpha,\sigma} \mapsto e^{i\theta} \hat{c}_{j,\alpha,\sigma}, \quad (26d)$$

$$\hat{U}(t) : \hat{c}_{j,\alpha,\sigma} \mapsto i\sigma_{\sigma,\nu}^y \hat{c}_{j,\alpha,\nu}, \quad (26e)$$

$$\hat{U}(m) : \hat{c}_{j,\alpha,\sigma} \mapsto i\tau_{\alpha,\rho}^x \sigma_{\sigma,\nu}^x \hat{c}_{j,\rho,\nu}, \quad (26f)$$

where  $\mathbf{K}$  is the complex conjugation and  $\sigma^i$  and  $\tau^i$  ( $i = x, y, z$ ) are Pauli matrices. Operators (26) form a global representation of symmetry group  $G_{f,\text{tot}}^{(1)}$ .

To demonstrate that the Hamiltonian (25) realizes a nontrivial FSPT phase, we consider the limit  $V \gg 1$ . The onsite repulsive interaction is then locally minimized in the two-dimensional local subspace spanned by the states

$$|1\rangle_j := \hat{c}_{j,\uparrow,1}^\dagger \hat{c}_{j,\downarrow,1}^\dagger |0\rangle, \quad |2\rangle_j := \hat{c}_{j,\uparrow,2}^\dagger \hat{c}_{j,\downarrow,2}^\dagger |0\rangle, \quad (27)$$

where  $|0\rangle$  is the vacuum state. Hence, at low-energies the 16-dimensional local fermionic Fock space at each site  $j$  is reduced to the 2D Hilbert space spanned by states  $|1\rangle_j$  and  $|2\rangle_j$ . In this subspace, the effective Hamiltonian becomes

$$\hat{H}_{\text{AIIM}} \Big|_{V \gg 1} \approx \hat{H}_{\text{ZXZ}} := - \sum_j \hat{Z}_j \hat{X}_{j+1} \hat{Z}_{j+2}, \quad (28)$$

where  $\hat{Z}_j$  and  $\hat{X}_j$  are effective degrees of freedom acting on the low-energy two-level Hilbert space (27). These operators are obtained by restricting the operators  $\hat{Z}_j^f$  and  $\hat{X}_j^f$  defined in Eq. (25c) to the low-energy subspace. They satisfy the  $\mathfrak{su}(2)$  algebra

$$[\hat{X}_j, \hat{Y}_k] = \delta_{j,k} 2i\hat{Z}_k, \quad \hat{Y}_j := i\hat{X}_j \hat{Z}_k. \quad (29)$$

The Hamiltonian  $\hat{H}_{\text{ZXZ}}$  is the cluster model introduced for spin-1/2 degrees of freedom in Ref. [102]. The ground state of this Hamiltonian realizes a 1D bosonic SPT phase protected by  $\mathbb{Z}_2^T \times \mathbb{Z}_2^M$  symmetry [103]. The protecting symmetries are represented by the operators

$$\hat{U}(t) \Big|_{V \gg 1} \approx \mathbf{K}, \quad \hat{U}(m) \Big|_{V \gg 1} \approx \prod_j \hat{X}_j, \quad (30)$$

which are the representations of TRS and mirror symmetries in Eq. (26) in the low-energy subspace. The AIIM low-energy Hamiltonian (28) has a non-degenerate and gapped ground state when periodic boundary conditions are imposed. Instead, with open boundary conditions, it has a fourfold ground state degeneracy owing to the existence of the operators

$$\{\hat{Z}_1, \hat{X}_1 \hat{Z}_2, \hat{Y}_1 \hat{Z}_2\}, \quad \{\hat{Z}_L, \hat{Z}_{L-1} \hat{X}_L, \hat{Z}_{L-1} \hat{Y}_L\} \quad (31)$$

localized at the boundaries and with the following properties: they commute with the Hamiltonian with open boundary conditions, form an  $\mathfrak{su}(2)$  algebra, and are odd under either  $\hat{U}(t)$  or  $\hat{U}(m)$  (which prevents them from being added to the Hamiltonian as perturbations). Therefore, each boundary supports a single gapless spin-1/2 degree of freedom. On the boundary degrees of freedom, the  $\mathbb{Z}_2^T \times \mathbb{Z}_2^M$  symmetry is realized projectively [94, 104].

The intrinsically interacting 1D FSPT phase realized by the AIIM model (25) can be understood as the bosonic SPT phase of the low-energy degrees of freedom that result from confinement of fermions due to interactions. In particular, the fermionic symmetry group  $G_{f,\text{tot}}^{(1)}$  reduces to the group  $\mathbb{Z}_2^T \times \mathbb{Z}_2^M$ . This is because in the low-energy subspace the  $U(1)^F$  symmetry trivializes to

$$\hat{U}(\theta) \Big|_{V \gg 1} \approx e^{i2\theta L}, \quad (32)$$

which is just a complex phase. Fermion parity symmetry,  $\hat{U}(\theta = \pi)$ , then just becomes identity, which is why the TRS and mirror symmetry subgroups  $\mathbb{Z}_4^T$  and  $\mathbb{Z}_4^M$  reduce to  $\mathbb{Z}_2^T$  and  $\mathbb{Z}_2^M$ , respectively. A gappable decoration of a 1D line by the AIIM Hamiltonian (25) then corresponds to the index  $\nu = 1$  introduced in Sec. II B, while a trivial decoration corresponds to  $\nu = 0$ .

To obtain a cFSPT where 1D Wyckoff patches are decorated by the AIIM phase, one has to ensure that the boundary modes of each 1D decoration are gapped out in the bulk. This is easily achieved by ensuring that the 1D decorations terminate at the same point, and share

the same mirror axis. Then, the boundary modes at a meeting point where a chain ends and another one begins are lifted by adding the term

$$\hat{Z}_{L-1}^f \hat{X}_L^f \hat{Z}_1^f + \hat{Z}_L^f \hat{X}_1^f \hat{Z}_2^f \quad (33)$$

to the Hamiltonian. In Eq. (33), operators with indices  $j \leq L$  belong to the first chain, and with  $j \geq 1$  to the second, and they are distinguished by non calligraphic and calligraphic symbols, respectively. If several pairs of 1D patches are related by rotation symmetry, as in the example of 6d and 6e decorations in  $p6mm$  [Fig. 2(f)], a set of rotationally symmetric copies of (33) are added to the full Hamiltonian.

#### IV. SIGNATURES OF CFSPT PHASES

We briefly address the question of how cFSPTs can be detected and distinguished by using ground state properties. We discuss the signatures of 0D and 1D decorations separately.

##### A. Signatures for 0D decorations

As we have discussed in Sec. II B nontrivial 0D decorations are characterized by symmetry charges localized at 0D Wyckoff patches. For a given 2D lattice with  $L$  unit-cells in total, related by translations, the many-body ground state of the full lattice  $|\Psi_L\rangle$  transforms as

$$\hat{U}(\theta) |\Psi_L\rangle = e^{i2L\theta \sum_{\alpha} n_{\alpha}} |\Psi_L\rangle, \quad (34a)$$

$$\hat{U}(r) |\Psi_L\rangle = \prod_{\alpha} r_{\alpha}^L |\Psi_L\rangle, \quad (34b)$$

$$\hat{U}(m) |\Psi_L\rangle = \prod_{\alpha} m_{\alpha}^L |\Psi_L\rangle, \quad (34c)$$

under  $U(1)$  transformations, rotations, and reflections, respectively, provided that the latter two are the symmetries of the lattice [Fig. 3(d)]. Hereby the index  $\alpha$  runs over the set of all 0D Wyckoff positions. Therefore, a partial but by far not exhaustive characterization of the cFSPT due to 0D decorations can be extracted from the particular sensitivity of the total symmetry charge on the system size  $L$ .

For cFSPTs that are only composed by 0D decorations, it was hinted in Refs. 100 and 105 that single-particle Green's function, often used to treat topological interacting systems by defining a “topological Hamiltonian” [105–109], fail in distinguishing between trivial and nontrivial symmetry charges of 0D decorations. However, in Ref. 100 it was shown that 0D decorations where the nontrivial symmetry charge is carried by two-particle entangled “clusters” of electrons can be distinguished by the two-particle Green's function, and a generalization to  $n$ -particle entanglement and  $n$ -particle Green's function

is suggested. In Ref. 101 an alternative scheme based on real space invariants was proposed.

When open boundary conditions are imposed, cFSPTs with only 0D decorations can support 0D topological boundary modes under certain conditions. This is possible if the 0D Wyckoff patch on which a MAL is located does not contain an atom itself. Then, one can define open boundary conditions that are globally preserving the relevant spatial symmetry and cut out a  $k$ -th of the Wyckoff patch with a MAL transforming nontrivially under  $C_k$  point group elements. A zero-energy excitation is bound to such a corner [Fig. 3(c)]. These modes are similar to those arising as “filling anomalies” in so-called obstructed atomic limits of noninteracting insulators [110–112].

##### B. Signatures for 1D decorations

For cFSPTs with nontrivial 1D decorations, the ground state  $|\Psi\rangle$  does not necessarily carry global charge under symmetries. However, the 1D FSPT phases acquire an expectation value for non-local string order parameters [113–115]. Namely, the analog of Eq. (34) is given by

$$\langle \Psi_L | \hat{O}_{\gamma} | \Psi_L \rangle \neq 0, \quad (35)$$

where  $\hat{O}_{\gamma}$  is a non-local string operator along a mirror symmetric line  $\gamma$  [Fig. 3(e)]. For the AIIM model introduced in Sec. III B, the string order parameter is given by

$$\hat{O}_{\gamma} := \hat{Z}_1^f \hat{Y}_2^f \hat{X}_3^f \hat{X}_4^f \cdots \hat{X}_{N-2}^f \hat{Y}_{N-1}^f \hat{Z}_N^f \quad (36)$$

in terms of the effective spin- $\frac{1}{2}$  degrees of freedom introduced in Eq. (25c), where  $j = 1, \dots, N$  labels the sites along the line  $\gamma$ . Alternatively, ground states of cFSPT phases can be detected by partial crystalline symmetry transformations [116–118].

There are two paradigmatic signatures of cFSPTs with nontrivial 1D decorations. First, when open boundary conditions are imposed, such cFSPTs feature gapless boundary states that are protected by both internal and crystalline symmetries. More precisely, as shown for the AIIM model in Sec. III B, each 1D decoration features an effective spin-1/2 degree of freedom when open boundary conditions are imposed. The boundary is then described by TRS invariant spin- $\frac{1}{2}$  chains with translation and (if present) additional crystalline symmetries. The protected gaplessness at the boundary can then be understood as a direct consequence of the generalized Lieb-Schultz-Mattis (LSM) theorems [79, 119–130] that apply to both effective spin-1/2 as well as the original fermionic degrees of freedom. Second, there are gapless boundary modes localized at lattice defects such as dislocations and disclinations (if rotation symmetry is present) [74]. This is because the otherwise gappable 1D decorations can no

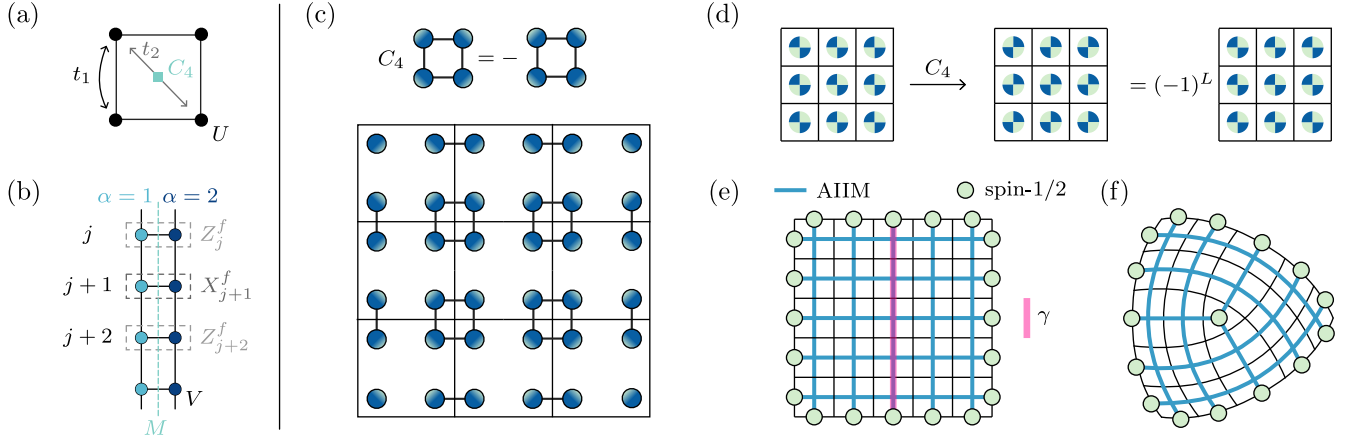


FIG. 3. (a), (b) Model Hamiltonians: (a) schematic of the Hubbard square with the four-fold rotation center marked by a blue square, and the two hopping terms, and Hubbard interaction indicated. (b) Schematic of the AIIM chain. The action of a single term in the Hamiltonian in Eq. (25) is shown, alongside the mirror-symmetry axis. In (a) and (b), the dots indicate spinful fermionic orbitals. (c)–(f) Distinguishing cFSPTs: (c) Square lattice ( $p4mm$ ) decorated by the rotation-odd Hubbard square ground state of Eq. (20) at the  $1b$  Wyckoff patch (the corner of the unit-cell). Since there are no physical sites at the  $1b$  Wyckoff patches, the lattice can be terminated by cutting through the decorations. This leads to a local two-fold degeneracy of the ground state at each corner, enforced by the combination of TRS, half-filling, and  $C_4$  symmetry of the full cluster. (d) Evaluation of the  $C_4$  charge at the  $1a$  Wyckoff position in  $p4mm$ . (e) Example of string order-parameter evaluation along the path  $\gamma$  (marked by the pink line) on 1D Wyckoff patches' decorations (marked by blue lines), which terminate with zero boundary modes for the nontrivial AIIM phase (marked by green dots). (f) A  $\pi/2$  disclination in the  $p4mm$  lattice leaves a gapless mode pinned at the disclination core.

longer be generically gapped at the defect center as dislocations and disclinations require the removal of appropriate 1D decorations. For example, in the  $p4mm$  wallpaper group, where four 1D Wyckoff patches meet at the center of the square, a  $\pi/2$  disclination, which amounts to “cutting” a  $\pi/2$  angle wide slice from the lattice, would prevent the hybridization of one of the gapless spin-1/2 degrees of freedom, therefore leading to a gapless mode located at the disclination core [Fig. 3(f)]. We refer to the mode pinned at the defect core as gapless, in the sense that it leads to a true ground state degeneracy, arising from local degrees of freedom.

## V. DISCUSSION

In summary, we have completed the classification of cFSPTs with TRS and  $U(1)$  charge-conservation for all the 17 wallpaper groups, and the result of the classification is summarized in Table I. We have adopted a real-space based construction first proposed in Refs. 78–82, and we have introduced the concept of Wyckoff patches as a natural prescription to obtain the unit-cell subdivision.

Due to the constructive nature of the classification procedure we adopted, each term appearing in the products of Table I can be precisely associated to a topological index, and each index in turn characterizes the decorations of a specific Wyckoff patch. The indices corresponding

to each entry of Table I are listed in Appendix B. For each wallpaper group the classification summarized in Table I always contains a  $\mathbb{Z}$  factor counting the total charge in the unit-cell, and a  $\mathbb{Z}_2$  factor always appearing at the end (colored in magenta) for the intrinsic 2D topological phase, which does not require crystalline symmetries to be protected. In addition to those, the wallpaper cFSPTs are classified by a series of  $\mathbb{Z}_n$  ( $n = 2, 3, 4, 6$ ) terms (colored in black) that describe the charge distribution within the unit-cell, and all the remaining  $\mathbb{Z}_2$  factors (colored in cyan) classify intrinsically interacting decorations. The latter correspond to either mirror and rotation charges, or to the AIIM phase, namely, the 1D non trivial cFSPT phase protected by mirror symmetry.

We remark that in our classification scheme, two Hamiltonians are in the same cFSPT phase only if they can be deformed to one another without symmetry breaking or gap closing. In particular, we do not allow stacking with “ancilla” degrees of freedom. This is in contrast to the classification of the so-called strong topological phases where stacking with a product state does not change the topological phase. Depending on the choice of ancillas some of the entries in Table I can be trivialized. For instance, all  $\mathbb{Z}$  entries corresponding to the  $U(1)$  charge per unit-cell, can be changed by stacking with charged ancillas. These phases correspond to the so-called fragile topological phases [131–134].

The ability to associate indices to real-space decorations is a rather powerful aspect of the real-space con-

struction, as it allows to not only extract the classification of cFSPTs, but also to construct fixed-point wave functions that lie in each of the phases predicted by the classification. These correspond to wave functions built by gluing together decorations matching the values of the topological indices describing the phase. We have both recalled and proposed model Hamiltonians for the realization of all the decorations necessary towards the construction of cFSPTs as their unique ground state, and finally we discussed possible approaches towards distinguishing these phases.

With this work, we hope to provide a tool that may support further study of interacting topological phases. In particular, we expect that this classification will be useful in characterizing more realistic Hamiltonian ground states that fall in the same symmetry classes as the cFSPTs analyzed here, namely, the one of interacting spin-orbit coupled interacting insulators, that do not undergo spontaneous symmetry breaking. The model Hamiltonians presented here may be a starting point to test the resilience of cFSPTs against disorder and perturbation away from the fixed-point wave functions. In addition, providing a classification to compare the results against, might be helpful in exploring the regime of validity of various methods and approaches used to detect and characterize cFSPTs.

## ACKNOWLEDGMENTS

We thank Apoorv Tiwari, Juven C. Wang, and Zheyang Wan for useful and extensive discussions in the early stages of this work. The authors acknowledge useful discussions with Max Geier and Christopher Mudry. M. O. S. acknowledges funding from the University of Zurich Forschungskredit (Grant No. FK-23-110). Ö. M. A. is supported by Swiss National Science Foundation (SNSF) under Grant No. P500PT-214429 and National Science Foundation (NSF) Grant No. DMR-2022428. T.N. and M. O. S. acknowledge support from the Swiss National Science Foundation (SNSF) through a Consolidator Grant (iTQC, TMC-2-213805) and through Grant No. 200021E-198011 as part of the FOR 5249 (QUAST) lead by the Deutsche Forschungsgemeinschaft (DFG, German Research Foundation).

## DATA AVAILABILITY

This publication is theoretical work that does not require supporting research data.

## Appendix A: Mirror charge equivalence

In Sec. IID of the main text, we derive the classification for the wallpaper group  $p6mm$  explicitly. There, we list the equivalences that reduce the set of independent topological indices. One of the equivalences comes from trivializing the  $m_{2b}$  mirror charge that classifies 0D decorations of the  $2b$  Wyckoff patches. This trivialization is possible because an odd number of Kramers' pairs can be brought to the  $2b$  patches through the  $6e$  Wyckoff patches [Fig. A4]. More formally, let us consider each  $2b$  Wyckoff patch to be decorated by a many-body state with the property

$$\hat{M}_x |\Psi_{2b}\rangle = m_{2b} |\Psi_{2b}\rangle, \quad (\text{A1})$$

where  $\hat{M}_x$  is the mirror operation with axis orthogonal to the  $x$  direction. From the  $1a$  patch, we can pull six Kramers' pairs along the  $6b$  lines [Fig. 2(g)], that can either be even or odd under mirror symmetry, without altering the  $m_{1a}$  charge. We choose to pull these six pairs such that they carry an odd charge under the onsite mirror of the  $6e$  patches,  $m_{6e} = -1$  [Fig. A4(a)]. Then, we pull these pairs close to the  $2b$  position, where we can write the wave function of these decorations along the  $6b$  patches as

$$|\Psi_{6b}\rangle = \hat{O}_{6e,1}^\dagger \hat{O}_{6e,2}^\dagger \hat{O}_{6e,3}^\dagger |0\rangle, \quad (\text{A2})$$

transforming as

$$\begin{aligned} M |\Psi_{6b}\rangle &= -\hat{O}_{6e,1}^\dagger \hat{O}_{6e,3}^\dagger \hat{O}_{6e,2}^\dagger |0\rangle = -|\Psi_{6b}\rangle, \\ C_3 |\Psi_{6b}\rangle &= \hat{O}_{6e,2}^\dagger \hat{O}_{6e,3}^\dagger \hat{O}_{6e,1}^\dagger |0\rangle = |\Psi_{6b}\rangle. \end{aligned} \quad (\text{A3})$$

The  $m_{2b}$  charge can then be neutralized by the process [Fig. A4(b)]

$$\begin{aligned} |\Psi_{2b}\rangle &\rightarrow |\Psi'_{2b}\rangle = \hat{O}_{6e,1}^\dagger \hat{O}_{6e,2}^\dagger \hat{O}_{6e,3}^\dagger |\Psi_{2b}\rangle, \\ M |\Psi'_{2b}\rangle &= -m_{2b} |\Psi'_{2b}\rangle. \end{aligned} \quad (\text{A4})$$

At the same time,  $m_{6e}$  also changes sign, therefore returning to its original value. Likewise, the inverse equivalence process is also allowed: the mirror charge at the  $m_{6e}$  positions can be neutralized by peeling  $3k$  Kramers' pairs from the  $2b$  position globally transforming oddly under the mirror symmetry of each  $6e$  Wyckoff position. Note that this particular process is possible due to the existence of an  $n$ -fold rotation in the site-symmetry group of  $2b$ , where  $n$  is odd. For even  $n$ , the mirror neutralization is in general not possible.



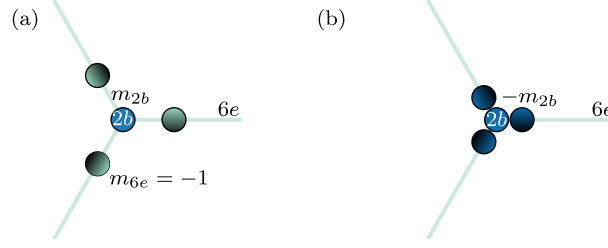


FIG. A4. Trivialization of the  $m_{2b}$  charge: (a) We move six mirror odd Kramers' pairs from the  $1a$  to the  $6e$  Wyckoff patches, which leads to a single Kramer's pair with mirror odd charge on each  $6e$  Wyckoff patch, such that  $m_{6e} = -1$  (assuming that initially  $m_{6e} = 1$ , without loss of generality). (b) We transfer three Kramers' pairs to each  $2b$  Wyckoff patch, which results into a change of sign of  $m_{2b}$  and trivializes  $m_{6e}$ .

## Appendix B: Classification of wallpaper group crystalline SPTs

In this appendix we provide the missing steps followed to obtain the cFSPTs classification for all the 17 wallpaper groups, namely, the various steps that lead to the entries in Table I. Details on the wallpaper groups, such as the coordinates of the Wyckoff positions and their site-symmetry groups, can be found for instance in Ref. 89, or online on the Bilbao Crystallographic Server website [135–137].

1. *Summary of wallpaper groups* Figure A5 depicts the unit-cell and Wyckoff positions for each of the 17 wallpaper groups. In all the panels, each Wyckoff position is represented as a dot, line or shaded quadrilateral for 0D, 1D or 2D Wyckoff patches, respectively.

2. *Enumeration of gappable decorations of wallpaper groups* Tables A1–A17 list the classification of gappable decorations for the 17 wallpaper groups, prior to taking into account any equivalence relations. The caption of each table indicates the wallpaper group to which the table refers to. For all of the Tables A1–A17, the column labels indicate the following:

- (i) “WP”: list of the Wyckoff position labels for the selected wallpaper group. These labels are conventionally defined [89], and are composed by a number (indicating the multiplicity of the Wyckoff position) followed by a letter (the labels follow the alphabetical order, starting from the most symmetric Wyckoff position).
- (ii) “dim”: Dimension of the Wyckoff patch corresponding to the Wyckoff position shown in the first column. In practice, the dimension is equal to the number of free parameters in the definition of the Wyckoff position coordinates.
- (iii) “site symm.”: Site-symmetry group of the Wyckoff position expressed in the Schoenflies notation.
- (iv) “ $G_{\text{spa}}$ ”: Site-symmetry group of the Wyckoff position written as internal spatial symmetry group, namely as groups of the form  $\mathbb{Z}_{2a}^F \rtimes \mathbb{Z}_{2b}^F$  ( $a = 1, 2, 3, 4, 6$  for  $a$ -fold rotation,  $b = 1, 2$  if mirror is not present or present, respectively). The individual factors contain the fermion parity, which motivates the superscript F. The fermion parity  $\mathbb{Z}_2^F$  has to be modded out when repeated more than once. This is described more in detail in Sec. IIB of the main text.
- (v) “Classification”: Classification for each Wyckoff patch, following the prescription of Table III in the main text, based on the entry in  $G_{\text{spa}}$ .
- (vi) “Gappable decorations”: subset of gappable decorations deduced from the “Classification” column. In particular, all 0D and 2D decorations are always gappable, while we only retain those 1D decorations whose endpoints meet in even number, and share the same mirror axis pair-wise.
- (vii) “Indices”: List of topological indices referred to the gappable decorations. Note that the order in which the indices are listed matches the order in which the groups are written in the product of groups in the column “Gappable decorations.”

For the topological indices, we follow the convention introduced in the main text. We summarize the convention here for convenience. For a Wyckoff patch whose Wyckoff position is labeled by  $wp$ , we indicate by the following:

1.  $n_{wp} \in \mathbb{Z}$  (or  $\mathbb{Z}_n$  with  $n = 2, 3, 4, 6$  after the reduction due to equivalence relations): Number of Kramers' pairs of 0D decorations at the Wyckoff patch  $wp$ .

2.  $r_{wp} \in \mathbb{Z}_2$ : Rotation charge of 0D decorations at the 0D  $wp$ .
3.  $m_{wp} \in \mathbb{Z}_2$ : Mirror charge of 0D decorations at the 0D or 1D Wyckoff patch  $wp$ .
4.  $\nu_{wp} \in \mathbb{Z}_2$ : 1D topological phase of 1D decorations at the 1D Wyckoff patch  $wp$ . This index classifies whether the 1D decorations are in the trivial phase, or the intrinsically interacting nontrivial phase which we call AIIM phase, discussed in Sec. III B of the main text.
5.  $x_{wp} \in \mathbb{Z}_2$ : 2D topological phase of 2D decorations at the 2D Wyckoff patch  $wp$ . This index counts whether the 2D decorations have helical edge states (nontrivial phase) or not (trivial phase).

When a list of such indices is written next to the product of groups the indices belong to, we keep the ordering consistent: For instance, the  $i$ th index listed in the column “Indices” belongs to the  $i$ th group of the product in “Gappable decorations.”

Note that while  $n_{wp}$  and  $x_{wp}$  are generically present for both interacting and noninteracting systems, instead the  $r_{wp}$ ,  $m_{wp}$ , and  $\nu_{wp}$  indices can assume nontrivial values only when interactions are present, i. e., their nontrivial values describe intrinsically interacting phases.

3. *Equivalence relations* In Appendix B 1, we list the equivalence relations for each of the 17 wallpaper groups, which allow to reduce the indices of the gappable decorations listed in Tables A1–A17. Equivalences are adiabatic and symmetry respecting deformations that allow to connect phases characterized by different topological indices without a gap closing occurring. These equivalences can either partially reduce, or fully trivialize, the group to which the indices originally belonged.

We separate equivalences into two sets:

- (i) Those obtained by symmetrically peeling off 0D decorations from a Wyckoff patch to another one, which only changes the value of the indices counting the number of Kramer’s pairs at the Wyckoff patches.
- (ii) Those obtained by symmetrically pulling 0D decorations carrying odd mirror charges from a 0D Wyckoff patch to a 1D Wyckoff patch (and vice versa). This type of equivalence results into a change of two of the Wyckoff patch mirror charges at once if the site-symmetry group of the 0D Wyckoff patch contains an odd-fold rotation, while only the 1D Wyckoff patch mirror charge is altered if the 0D Wyckoff patch only has an odd-fold rotation symmetry.

Note that when two mirror charges flip sign at the same time, such an equivalence leaves out as a topological index the overall parity of the mirror charges. We call this index  $m \equiv m_{1a}m_{1b}m_{1c}m_{3d}$  in the case of wallpaper group  $p3m1$  (No. 14), and  $m \equiv m_{1a}m_{1b}$  for the wallpaper group  $p31m$  (No. 15).

We indicate each process by writing the changes in the affected indices, while it is assumed that all the other indices are left unchanged. For example, the process described in Eq. (13) of the main text, for the wallpaper group  $p6mm$ ,

$$(n_{1a}, n_{2b}) \rightarrow (n_{1a} - 6k, n_{2b} + 3k), \quad (\text{B1})$$

is listed in Appendix B 1 as

$$n_{1a} - 6k, n_{2b} + 3k, \quad (\text{B2})$$

and a mirror charge trivialization of the type  $m_{6e} \rightarrow -m_{6e}$  is listed as  $-m_{6e}$ .

After listing the equivalence processes, for every wallpaper group we then explicitly show the reduction of the indices occurring due to the equivalence processes. We write on the left-hand side of the arrow “ $\rightarrow$ ” the original indices with their classification (omitting those indices that are left unchanged by all the equivalence relations), and on the right hand side the reduced classification. In particular, indices that are fully trivialized, namely, whose group becomes  $\mathbb{Z}_1$  after taking into account equivalence relations, are omitted on the right hand side of the arrow.

4. *Classification of cFSPTs in wallpaper groups with corresponding indices.* Table A18 lists the cFSPT classification obtained for each wallpaper group, alongside the indices corresponding to each factor in the classification. The first two columns identify the wallpaper group through its number (“No.”) and label (“Wallpaper”). The “Classification” column lists the full (interacting) classification, while the “Noninteracting classification” column shows the classification retained in the absence of interactions. The last column, “Indices”, explicitly lists the topological indices that are associated to the (interacting) classification. Once more, the ordering of the indices listed in the “Indices” column and the groups appearing in the product in the “Classification” column is consistent.

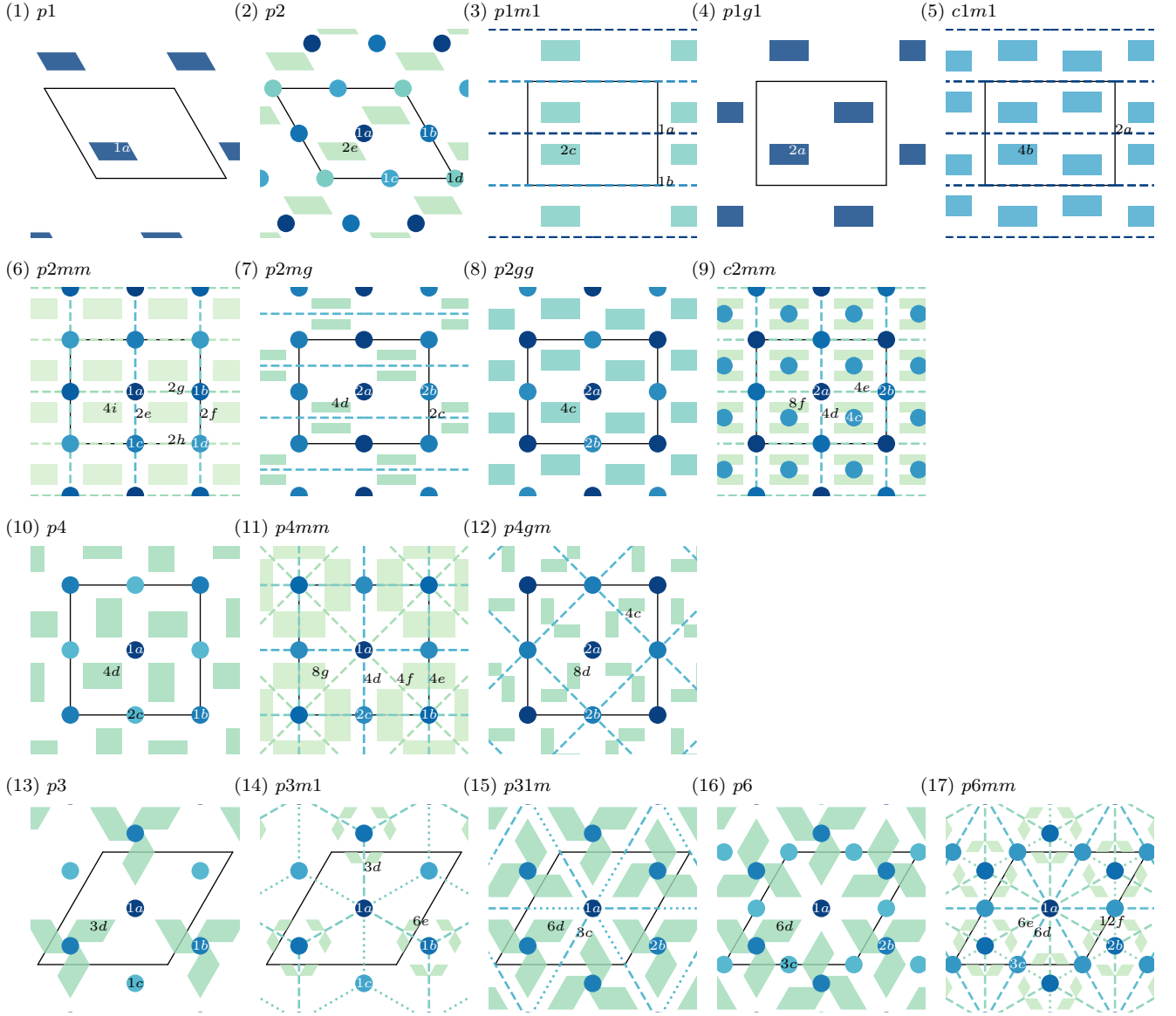


FIG. A5. Representation of the Wyckoff patches for the 17 wallpaper groups. The panels are labeled by the Wallpaper group's number and label. Each Wyckoff patch is labeled by the Wyckoff position from which it originates, and it is represented according to its dimension: 0D Wyckoff patches are marked by dots, 1D by dashed or dotted lines, and 2D by shaded quadrilateral regions. In each panel, a single unit-cell is marked by black lines. For the wallpaper groups Nos. 14, 15 and 17, dashed and dotted lines showcase how some of the 1D patches can be decorated in different ways: 1D decorations can be glued along dashed lines only, dotted lines only, or along both at the same time.

### 1. Enumeration of gappable decorations and equivalences

In this section, we list all the equivalence relations for each 993 of the wallpaper groups [Sec. B].

#### No. 1 ( $p1$ )

WP	dim	site symm.	$G_{\text{spa}}$	Classification	Gappable decorations	Indices
1a	2D	$C_1$	$\mathbb{Z}_1$	$\mathbb{Z} \times \mathbb{Z}_2$	$\mathbb{Z} \times \mathbb{Z}_2$	$(n_{1a}, x_{1a})$

TABLE A1. No. 1,  $p1$ .

No equivalence relations.

#### No. 2 ( $p2$ )

WP	dim	site symm.	$G_{\text{spa}}$	Classification	Gappable decorations	Indices
1a	0D	$C_2$	$\mathbb{Z}_4^F$	$\mathbb{Z} \times \mathbb{Z}_2$	$\mathbb{Z} \times \mathbb{Z}_2$	$(n_{1a}, r_{1a})$
1b	0D	$C_2$	$\mathbb{Z}_4^F$	$\mathbb{Z} \times \mathbb{Z}_2$	$\mathbb{Z} \times \mathbb{Z}_2$	$(n_{1b}, r_{1b})$
1c	0D	$C_2$	$\mathbb{Z}_4^F$	$\mathbb{Z} \times \mathbb{Z}_2$	$\mathbb{Z} \times \mathbb{Z}_2$	$(n_{1c}, r_{1c})$
1d	0D	$C_2$	$\mathbb{Z}_4^F$	$\mathbb{Z} \times \mathbb{Z}_2$	$\mathbb{Z} \times \mathbb{Z}_2$	$(n_{1d}, r_{1d})$
2e	2D	$C_1$	$\mathbb{Z}_1$	$\mathbb{Z} \times \mathbb{Z}_2$	$\mathbb{Z} \times \mathbb{Z}_2$	$(n_{2e}, x_{2e})$

TABLE A2. No. 2,  $p2$ .

Equivalence relations: Type (i)

$$n_{1a} - 2k, n_{1b} + 2k \quad (\text{B3})$$

$$n_{1a} - 2k, n_{1c} + 2k \quad (\text{B4})$$

$$n_{1a} - 2k, n_{1d} + 2k \quad (\text{B5})$$

$$n_{1a} - 2k, n_{2e} + k, \quad (\text{B6})$$

Reduced indices:

$$(n_{1a}, n_{1b}, n_{1c}, n_{1d}, n_{2e}) \in \mathbb{Z}^5 \rightarrow (n_{1a}, n_{1b}, n_{1c}, n_{1d}) \in (\mathbb{Z}_2)^4 \quad (\text{B7})$$

#### No. 3 ( $p1m1$ )

WP	dim	site symm.	$G_{\text{spa}}$	Classification	Gappable decorations	Indices
1a	1D	$C_s$	$\mathbb{Z}_4^F$	$\mathbb{Z} \times \mathbb{Z}_2 \times \mathbb{Z}_2$	$\mathbb{Z} \times \mathbb{Z}_2 \times \mathbb{Z}_2$	$(n_{1a}, m_{1a}, \nu_{1a})$
1b	1D	$C_s$	$\mathbb{Z}_4^F$	$\mathbb{Z} \times \mathbb{Z}_2 \times \mathbb{Z}_2$	$\mathbb{Z} \times \mathbb{Z}_2 \times \mathbb{Z}_2$	$(n_{1b}, m_{1b}, \nu_{1b})$
2c	2D	$C_1$	$\mathbb{Z}_1$	$\mathbb{Z} \times \mathbb{Z}_2$	$\mathbb{Z} \times \mathbb{Z}_2$	$(n_{2c}, x_{2c})$

TABLE A3. No. 3,  $p1m1$ .

Equivalence relations: Type (i)

$$n_{1a} - 2k, n_{1b} + 2k \quad (\text{B8})$$

$$n_{1a} - 2k, n_{2c} + k. \quad (\text{B9})$$

Reduced indices:

$$(n_{1a}, n_{1b}, n_{2c}) \in \mathbb{Z}^3 \rightarrow (n_{1a}, n_{1b}) \in (\mathbb{Z}_2)^2 \quad (\text{B10})$$



**No. 4** ( $p1g1$ )

WP	dim	site symm.	$G_{\text{spa}}$	Classification	Gappable decorations	Indices
$2a$	2D	$C_1$	$\mathbb{Z}_1^F$	$\mathbb{Z} \times \mathbb{Z}_2$	$\mathbb{Z} \times \mathbb{Z}_2$	$(n_{2a}, x_{2a})$

TABLE A4. No. 4,  $p1g1$ .

No equivalence relations.

**No. 5** ( $c1m1$ )

WP	dim	site symm.	$G_{\text{spa}}$	Classification	Gappable decorations	Indices
$2a$	1D	$C_s$	$\mathbb{Z}_4^F$	$\mathbb{Z} \times \mathbb{Z}_2 \times \mathbb{Z}_2$	$\mathbb{Z} \times \mathbb{Z}_2 \times \mathbb{Z}_2$	$(n_{2a}, m_{2a}, \nu_{2a})$
$4b$	2D	$C_1$	$\mathbb{Z}_1$	$\mathbb{Z} \times \mathbb{Z}_2$	$\mathbb{Z} \times \mathbb{Z}_2$	$(n_{4b}, x_{4b})$

TABLE A5. No. 5,  $c1m1$ .

Equivalence relations: Type (i)

$$n_{2a} - 2k, n_{4b} + k. \quad (\text{B11})$$

Reduced indices:

$$(n_{2a}, n_{4b}) \in \mathbb{Z}^2 \rightarrow n_{2a} \in \mathbb{Z}_2 \quad (\text{B12})$$

**No. 6** ( $p2mm$ )

WP	dim	site symm.	$G_{\text{spa}}$	Classification	Gappable decorations	Indices
$1a$	0D	$C_{2v}$	$\mathbb{Z}_4^F \rtimes \mathbb{Z}_4^F / \mathbb{Z}_2^F$	$\mathbb{Z} \times \mathbb{Z}_2 \times \mathbb{Z}_2$	$\mathbb{Z} \times \mathbb{Z}_2 \times \mathbb{Z}_2$	$(n_{1a}, r_{1a}, m_{1a})$
$1b$	0D	$C_{2v}$	$\mathbb{Z}_4^F \rtimes \mathbb{Z}_4^F / \mathbb{Z}_2^F$	$\mathbb{Z} \times \mathbb{Z}_2 \times \mathbb{Z}_2$	$\mathbb{Z} \times \mathbb{Z}_2 \times \mathbb{Z}_2$	$(n_{1b}, r_{1b}, m_{1b})$
$1c$	0D	$C_{2v}$	$\mathbb{Z}_4^F \rtimes \mathbb{Z}_4^F / \mathbb{Z}_2^F$	$\mathbb{Z} \times \mathbb{Z}_2 \times \mathbb{Z}_2$	$\mathbb{Z} \times \mathbb{Z}_2 \times \mathbb{Z}_2$	$(n_{1c}, r_{1c}, m_{1c})$
$1d$	0D	$C_{2v}$	$\mathbb{Z}_4^F \rtimes \mathbb{Z}_4^F / \mathbb{Z}_2^F$	$\mathbb{Z} \times \mathbb{Z}_2 \times \mathbb{Z}_2$	$\mathbb{Z} \times \mathbb{Z}_2 \times \mathbb{Z}_2$	$(n_{1d}, r_{1d}, m_{1d})$
$2e$	1D	$C_s$	$\mathbb{Z}_4^F$	$\mathbb{Z} \times \mathbb{Z}_2 \times \mathbb{Z}_2$	$\mathbb{Z} \times \mathbb{Z}_2 \times \mathbb{Z}_2$	$(n_{2e}, m_{2e}, \nu_{2e})$
$2f$	1D	$C_s$	$\mathbb{Z}_4^F$	$\mathbb{Z} \times \mathbb{Z}_2 \times \mathbb{Z}_2$	$\mathbb{Z} \times \mathbb{Z}_2 \times \mathbb{Z}_2$	$(n_{2f}, m_{2f}, \nu_{2f})$
$2g$	1D	$C_s$	$\mathbb{Z}_4^F$	$\mathbb{Z} \times \mathbb{Z}_2 \times \mathbb{Z}_2$	$\mathbb{Z} \times \mathbb{Z}_2 \times \mathbb{Z}_2$	$(n_{2g}, m_{2g}, \nu_{2g})$
$2h$	1D	$C_s$	$\mathbb{Z}_4^F$	$\mathbb{Z} \times \mathbb{Z}_2 \times \mathbb{Z}_2$	$\mathbb{Z} \times \mathbb{Z}_2 \times \mathbb{Z}_2$	$(n_{2h}, m_{2h}, \nu_{2h})$
$4i$	2D	$C_1$	$\mathbb{Z}_1$	$\mathbb{Z} \times \mathbb{Z}_2$	$\mathbb{Z} \times \mathbb{Z}_2$	$(n_{4i}, x_{4i})$

TABLE A6. No. 6,  $p2mm$ .

Equivalence relations: Type (i)

$$n_{1a} - 2k, n_{1b} + 2k \quad (\text{B13})$$

$$n_{1a} - 2k, n_{1c} + 2k \quad (\text{B14})$$

$$n_{1a} - 2k, n_{1d} + 2k \quad (\text{B15})$$

$$n_{1a} - 2k, n_{2e} + k \quad (\text{B16})$$

$$n_{1a} - 2k, n_{2f} + k \quad (\text{B17})$$

$$n_{1a} - 2k, n_{2g} + k \quad (\text{B18})$$

$$n_{1a} - 2k, n_{2h} + k \quad (\text{B19})$$

$$n_{1a} - 2k, n_{4i} + k. \quad (\text{B20})$$

Type (ii)

$$-m_{2e} \quad (\text{B21})$$

$$-m_{2g} \quad (\text{B22})$$

$$-m_{2f} \quad (\text{B23})$$

$$-m_{2h}. \quad (\text{B24})$$

Reduced indices:

$$(n_{1a}, n_{1b}, n_{1c}, n_{1d}, n_{2e}, n_{2f}, n_{2g}, n_{2h}, n_{4i}, m_{2e}, m_{2f}, m_{2g}, m_{2h}) \in \mathbb{Z}^9 \times (\mathbb{Z}_2)^4 \quad (\text{B25})$$

$$\rightarrow (n_{1a}, n_{1b}, n_{1c}, n_{1d}) \in (\mathbb{Z}_2)^4 \quad (\text{B26})$$

**No. 7** ( $p2mg$ )

WP	dim	site symm.	$G_{\text{spa}}$	Classification	Gappable decorations	Indices
2a	0D	$C_2$	$\mathbb{Z}_4^F$	$\mathbb{Z} \times \mathbb{Z}_2$	$\mathbb{Z} \times \mathbb{Z}_2$	$(n_{2a}, r_{2a})$
2b	0D	$C_2$	$\mathbb{Z}_4^F$	$\mathbb{Z} \times \mathbb{Z}_2$	$\mathbb{Z} \times \mathbb{Z}_2$	$(n_{2b}, r_{2b})$
2c	1D	$C_s$	$\mathbb{Z}_4^F$	$\mathbb{Z} \times \mathbb{Z}_2 \times \mathbb{Z}_2$	$\mathbb{Z} \times \mathbb{Z}_2 \times \mathbb{Z}_2$	$(n_{2c}, m_{2c}, \nu_{2c})$
4d	2D	$C_1$	$\mathbb{Z}_1$	$\mathbb{Z} \times \mathbb{Z}_2$	$\mathbb{Z} \times \mathbb{Z}_2$	$(n_{4d}, x_{4d})$

TABLE A7. No. 7,  $p2mg$ .

Equivalence relations: Type (i)

$$n_{2a} - 2k, n_{2b} + 2k \quad (\text{B27})$$

$$n_{2a} - 2k, n_{2c} + 2k \quad (\text{B28})$$

$$n_{2a} - 2k, n_{4b} + k. \quad (\text{B29})$$

Reduced indices:

$$(n_{2a}, n_{2b}, n_{2c}, n_{4d}) \in \mathbb{Z}^4 \rightarrow (n_{2a}, n_{2b}, n_{2c}) \in (\mathbb{Z}_2)^3 \quad (\text{B30})$$

**No. 8** ( $p2gg$ )

WP	dim	site symm.	$G_{\text{spa}}$	Classification	Gappable decorations	Indices
2a	0D	$C_2$	$\mathbb{Z}_4^F$	$\mathbb{Z} \times \mathbb{Z}_2$	$\mathbb{Z} \times \mathbb{Z}_2$	$(n_{2a}, r_{2a})$
2b	0D	$C_2$	$\mathbb{Z}_4^F$	$\mathbb{Z} \times \mathbb{Z}_2$	$\mathbb{Z} \times \mathbb{Z}_2$	$(n_{2b}, r_{2b})$
4c	2D	$C_1$	$\mathbb{Z}_1$	$\mathbb{Z} \times \mathbb{Z}_2$	$\mathbb{Z} \times \mathbb{Z}_2$	$(n_{4c}, x_{4c})$

TABLE A8. No. 8,  $p2gg$ .

Equivalence relations: Type (i)

$$n_{2a} - 2k, n_{2b} + 2k \quad (\text{B31})$$

$$n_{2a} - 2k, n_{4c} + k. \quad (\text{B32})$$

Reduced indices:

$$(n_{2a}, n_{2b}, n_{4c}) \in \mathbb{Z}^3 \rightarrow (n_{2a}, n_{2b}) \in (\mathbb{Z}_2)^2 \quad (\text{B33})$$

**No. 9** ( $c2mm$ )

WP	dim	site symm.	$G_{\text{spa}}$	Classification	Gappable decorations	Indices
2a	0D	$C_{2v}$	$\mathbb{Z}_4^F \rtimes \mathbb{Z}_4^F / \mathbb{Z}_2^F$	$\mathbb{Z} \times \mathbb{Z}_2 \times \mathbb{Z}_2$	$\mathbb{Z} \times \mathbb{Z}_2 \times \mathbb{Z}_2$	$(n_{2a}, r_{2a}, m_{2a})$
2b	0D	$C_{2v}$	$\mathbb{Z}_4^F \rtimes \mathbb{Z}_4^F / \mathbb{Z}_2^F$	$\mathbb{Z} \times \mathbb{Z}_2 \times \mathbb{Z}_2$	$\mathbb{Z} \times \mathbb{Z}_2 \times \mathbb{Z}_2$	$(n_{2b}, r_{2b}, m_{2b})$
4c	0D	$C_2$	$\mathbb{Z}_4^F$	$\mathbb{Z} \times \mathbb{Z}_2$	$\mathbb{Z} \times \mathbb{Z}_2$	$(n_{4c}, r_{4c})$
4d	1D	$C_s$	$\mathbb{Z}_4^F$	$\mathbb{Z} \times \mathbb{Z}_2 \times \mathbb{Z}_2$	$\mathbb{Z} \times \mathbb{Z}_2 \times \mathbb{Z}_2$	$(n_{4d}, m_{4d}, \nu_{4d})$
4e	1D	$C_s$	$\mathbb{Z}_4^F$	$\mathbb{Z} \times \mathbb{Z}_2 \times \mathbb{Z}_2$	$\mathbb{Z} \times \mathbb{Z}_2 \times \mathbb{Z}_2$	$(n_{4e}, m_{4e}, \nu_{4e})$
8f	2D	$C_1$	$\mathbb{Z}_1$	$\mathbb{Z} \times \mathbb{Z}_2$	$\mathbb{Z} \times \mathbb{Z}_2$	$(n_{8f}, x_{8f})$

TABLE A9. No. 9,  $c2mm$ .

Equivalence relations: Type (i)

$$n_{2a} - 2k, n_{2b} + 2k \quad (\text{B34})$$

$$n_{2a} - 4k, n_{4c} + 2k \quad (\text{B35})$$

$$n_{2a} - 2k, n_{4d} + k \quad (\text{B36})$$

$$n_{2a} - 2k, n_{4e} + k \quad (\text{B37})$$

$$n_{2a} - 4k, n_{8f} + k. \quad (\text{B38})$$

Type (ii)

$$-m_{4e} \quad (\text{B39})$$

$$-m_{4d}. \quad (\text{B40})$$

Reduced indices:

$$(n_{2a}, n_{2b}, n_{4c}, n_{4d}, n_{4e}, n_{8f}, m_{4e}, m_{4d}) \in \mathbb{Z}^6 \times (\mathbb{Z}_2)^2 \rightarrow (n_{2a}, n_{2b}n_{4c}) \in (\mathbb{Z}_2)^3 \quad (\text{B41})$$

**No. 10** ( $p4$ )

WP	dim	site symm.	$G_{\text{spa}}$	Classification	Gappable decorations	Indices
1a	0D	$C_4$	$\mathbb{Z}_8^F$	$\mathbb{Z} \times \mathbb{Z}_2$	$\mathbb{Z} \times \mathbb{Z}_2$	$(n_{1a}, r_{1a})$
1b	0D	$C_4$	$\mathbb{Z}_8^F$	$\mathbb{Z} \times \mathbb{Z}_2$	$\mathbb{Z} \times \mathbb{Z}_2$	$(n_{1b}, r_{1b})$
2c	0D	$C_2$	$\mathbb{Z}_4^F$	$\mathbb{Z} \times \mathbb{Z}_2$	$\mathbb{Z} \times \mathbb{Z}_2$	$(n_{2c}, r_{2c})$
4d	2D	$C_1$	$\mathbb{Z}_1$	$\mathbb{Z} \times \mathbb{Z}_2$	$\mathbb{Z} \times \mathbb{Z}_2$	$(n_{4d}, x_{4d})$

TABLE A10. No. 10,  $p4$ .

Equivalence relations: Type (i)

$$n_{1a} - 4k, n_{1b} + 4k \quad (\text{B42})$$

$$n_{1a} - 4k, n_{2c} + 2k \quad (\text{B43})$$

$$n_{1a} - 4k, n_{4d} + k. \quad (\text{B44})$$

Reduced indices:

$$(n_{1a}, n_{1b}, n_{2c}, n_{4d}) \in \mathbb{Z}^4 \rightarrow (n_{1a}, n_{1b}, n_{2c}) \in (\mathbb{Z}_4)^2 \times \mathbb{Z}_2 \quad (\text{B45})$$

**No. 11** ( $p4mm$ )

WP	dim	site symm.	$G_{\text{spa}}$	Classification	Gappable decorations	Indices
1a	0D	$C_{4v}$	$\mathbb{Z}_8^F \rtimes \mathbb{Z}_4^F / \mathbb{Z}_2^F$	$\mathbb{Z} \times \mathbb{Z}_2 \times \mathbb{Z}_2$	$\mathbb{Z} \times \mathbb{Z}_2 \times \mathbb{Z}_2$	$(n_{1a}, r_{1a}, m_{1a})$
1b	0D	$C_{4v}$	$\mathbb{Z}_8^F \rtimes \mathbb{Z}_4^F / \mathbb{Z}_2^F$	$\mathbb{Z} \times \mathbb{Z}_2 \times \mathbb{Z}_2$	$\mathbb{Z} \times \mathbb{Z}_2 \times \mathbb{Z}_2$	$(n_{1b}, r_{1b}, m_{1b})$
2c	0D	$C_{2v}$	$\mathbb{Z}_4^F \rtimes \mathbb{Z}_4^F / \mathbb{Z}_2^F$	$\mathbb{Z} \times \mathbb{Z}_2 \times \mathbb{Z}_2$	$\mathbb{Z} \times \mathbb{Z}_2 \times \mathbb{Z}_2$	$(n_{2c}, r_{2c}, m_{2c})$
4d	1D	$C_s$	$\mathbb{Z}_4^F$	$\mathbb{Z} \times \mathbb{Z}_2 \times \mathbb{Z}_2$	$\mathbb{Z} \times \mathbb{Z}_2 \times \mathbb{Z}_2$	$(n_{4d}, m_{4d}, \nu_{4d})$
4e	1D	$C_s$	$\mathbb{Z}_4^F$	$\mathbb{Z} \times \mathbb{Z}_2 \times \mathbb{Z}_2$	$\mathbb{Z} \times \mathbb{Z}_2 \times \mathbb{Z}_2$	$(n_{4e}, m_{4e}, \nu_{4e})$
4f	1D	$C_s$	$\mathbb{Z}_4^F$	$\mathbb{Z} \times \mathbb{Z}_2 \times \mathbb{Z}_2$	$\mathbb{Z} \times \mathbb{Z}_2 \times \mathbb{Z}_2$	$(n_{4f}, m_{4f}, \nu_{4f})$
8g	2D	$C_1$	$\mathbb{Z}_1$	$\mathbb{Z} \times \mathbb{Z}_2$	$\mathbb{Z} \times \mathbb{Z}_2$	$(n_{8g}, x_{8g})$

TABLE A11. No. 11,  $p4mm$ .

Equivalence relations: Type (i)

$$n_{1a} - 4k, n_{1b} + 4k \quad (\text{B46})$$

$$n_{1a} - 4k, n_{2c} + 2k \quad (\text{B47})$$

$$n_{1a} - 4k, n_{4d} + k \quad (\text{B48})$$

$$n_{1a} - 4k, n_{4e} + k \quad (\text{B49})$$

$$n_{1a} - 4k, n_{4f} + k \quad (\text{B50})$$

$$n_{1a} - 4k, n_{8g} + k. \quad (\text{B51})$$

Type (ii)

$$-m_{4d} \quad (\text{B52})$$

$$-m_{4e} \quad (\text{B53})$$

$$-m_{4f}. \quad (\text{B54})$$

Reduced indices:

$$(n_{1a}, n_{1b}, n_{2c}, n_{4d}, n_{4e}, n_{4f}, n_{8g}, m_{4d}, m_{4e}, m_{4f}) \in \mathbb{Z}^7 \times (\mathbb{Z}_2)^3 \rightarrow (n_{1a}, n_{1b}, n_{2c}) \in (\mathbb{Z}_4)^2 \times \mathbb{Z}_2 \quad (\text{B55})$$

**No. 12** ( $p4gm$ )

WP	dim	site symm.	$G_{\text{spa}}$	Classification	Gappable decorations	Indices
2a	0D	$C_4$	$\mathbb{Z}_8^F$	$\mathbb{Z} \times \mathbb{Z}_2$	$\mathbb{Z} \times \mathbb{Z}_2$	$(n_{2a}, r_{2a})$
2b	0D	$C_{2v}$	$\mathbb{Z}_4^F \rtimes \mathbb{Z}_4^F / \mathbb{Z}_2^F$	$\mathbb{Z} \times \mathbb{Z}_2 \times \mathbb{Z}_2$	$\mathbb{Z} \times \mathbb{Z}_2 \times \mathbb{Z}_2$	$(n_{2b}, r_{2b}, m_{2b})$
4c	1D	$C_s$	$\mathbb{Z}_4^F$	$\mathbb{Z} \times \mathbb{Z}_2 \times \mathbb{Z}_2$	$\mathbb{Z} \times \mathbb{Z}_2 \times \mathbb{Z}_2$	$(n_{4c}, m_{4c}, \nu_{4c})$
8d	2D	$C_1$	$\mathbb{Z}_1$	$\mathbb{Z} \times \mathbb{Z}_2$	$\mathbb{Z} \times \mathbb{Z}_2$	$(n_{8d}, x_{8d})$

TABLE A12. No. 12,  $p4gm$ .

Equivalence relations: Type (i)

$$n_{2a} - 4k, n_{2b} + 4k \quad (\text{B56})$$

$$n_{2a} - 4k, n_{4c} + 2k \quad (\text{B57})$$

$$n_{2a} - 4k, n_{8d} + k. \quad (\text{B58})$$

Type (ii)

$$-m_{4c}. \quad (\text{B59})$$

Reduced indices:

$$(n_{2a}, n_{2b}, n_{4c}, n_{8d}, m_{4c}) \in \mathbb{Z}^4 \times \mathbb{Z}_2 \rightarrow (n_{2a}, n_{2b}, n_{4c}) \in (\mathbb{Z}_4)^2 \times \mathbb{Z}_2 \quad (\text{B60})$$



**No. 13** ( $p3$ )

WP	dim	site symm.	$G_{\text{spa}}$	Classification	Gappable decorations	Indices
1a	0D	$C_3$	$\mathbb{Z}_6^F$	$\mathbb{Z}$	$\mathbb{Z}$	$n_{1a}$
1b	0D	$C_3$	$\mathbb{Z}_6^F$	$\mathbb{Z}$	$\mathbb{Z}$	$n_{1b}$
1c	0D	$C_3$	$\mathbb{Z}_6^F$	$\mathbb{Z}$	$\mathbb{Z}$	$n_{1c}$
3d	2D	$C_1$	$\mathbb{Z}_1$	$\mathbb{Z} \times \mathbb{Z}_2$	$\mathbb{Z} \times \mathbb{Z}_2$	$(n_{3d}, x_{3d})$

TABLE A13. No. 13,  $p3$ .

Equivalence relations: Type (i)

$$n_{1a} - 3k, n_{1b} + 3k \quad (\text{B61})$$

$$n_{1a} - 3k, n_{1c} + 3k \quad (\text{B62})$$

$$n_{1a} - 3k, n_{3d} + k. \quad (\text{B63})$$

Reduced indices:

$$(n_{1a}, n_{1b}, n_{1c}, n_{3d}) \in (\mathbb{Z})^4 \rightarrow (n_{1a}, n_{1b}, n_{1c}) \in (\mathbb{Z}_3)^3 \quad (\text{B64})$$

**No. 14** ( $p3m1$ )

WP	dim	site symm.	$G_{\text{spa}}$	Classification	Gappable decorations	Indices
1a	0D	$C_{3v}$	$\mathbb{Z}_6^F \rtimes \mathbb{Z}_4^F / \mathbb{Z}_2^F$	$\mathbb{Z} \times \mathbb{Z}_2$	$\mathbb{Z} \times \mathbb{Z}_2$	$(n_{1a}, m_{1a})$
1b	0D	$C_{3v}$	$\mathbb{Z}_6^F \rtimes \mathbb{Z}_4^F / \mathbb{Z}_2^F$	$\mathbb{Z} \times \mathbb{Z}_2$	$\mathbb{Z} \times \mathbb{Z}_2$	$(n_{1b}, m_{1b})$
1c	0D	$C_{3v}$	$\mathbb{Z}_6^F \rtimes \mathbb{Z}_4^F / \mathbb{Z}_2^F$	$\mathbb{Z} \times \mathbb{Z}_2$	$\mathbb{Z} \times \mathbb{Z}_2$	$(n_{1c}, m_{1c})$
3d	1D	$C_s$	$\mathbb{Z}_4^F$	$\mathbb{Z} \times \mathbb{Z}_2 \times \mathbb{Z}_2$	$\mathbb{Z} \times \mathbb{Z}_2 \times \mathbb{Z}_2$	$(n_{3d}, m_{3d}, \nu_{3d})$
6e	2D	$C_1$	$\mathbb{Z}_1$	$\mathbb{Z} \times \mathbb{Z}_2$	$\mathbb{Z} \times \mathbb{Z}_2$	$(n_{6e}, x_{6e})$

TABLE A14. No. 14,  $p3m1$ .

Equivalence relations: Type (i)

$$n_{1a} - 3k, n_{1b} + 3k \quad (\text{B65})$$

$$n_{1a} - 3k, n_{1c} + 3k \quad (\text{B66})$$

$$n_{1a} - 3k, n_{3d} + k \quad (\text{B67})$$

$$n_{1a} - 6k, n_{6e} + k. \quad (\text{B68})$$

Type (ii)

$$-m_{1a}, -m_{3d} \quad (\text{B69})$$

$$-m_{1b}, -m_{3d} \quad (\text{B70})$$

$$-m_{1c}, -m_{3d}. \quad (\text{B71})$$

Reduced indices:

$$\begin{aligned} (n_{1a}, n_{1b}, n_{1c}, n_{3d}, n_{6e}, m_{1a}, m_{1b}, m_{1c}, m_{3d}) &\in (\mathbb{Z})^5 \times (\mathbb{Z}_2)^4 \\ &\rightarrow (n_{1a}, n_{1b}, n_{1c}, m \equiv m_{1a}m_{1b}m_{1c}m_{3d}) \in (\mathbb{Z}_3)^3 \times \mathbb{Z}_2 \end{aligned} \quad (\text{B72})$$

**No. 15** ( $p31m$ )

WP	dim	site symm.	$G_{\text{spa}}$	Classification	Gappable decorations	Indices
1a	0D	$C_{3v}$	$\mathbb{Z}_6^F \rtimes \mathbb{Z}_4^F / \mathbb{Z}_2^F$	$\mathbb{Z} \times \mathbb{Z}_2$	$\mathbb{Z} \times \mathbb{Z}_2$	$(n_{1a}, m_{1a})$
2b	0D	$C_3$	$\mathbb{Z}_6^F$	$\mathbb{Z}$	$\mathbb{Z}$	$n_{2b}$
3c	1D	$C_s$	$\mathbb{Z}_2^F$	$\mathbb{Z} \times \mathbb{Z}_2 \times \mathbb{Z}_2$	$\mathbb{Z} \times \mathbb{Z}_2 \times \mathbb{Z}_2$	$(n_{3c}, m_{3c}, \nu_{3c})$
6d	2D	$C_1$	$\mathbb{Z}_1$	$\mathbb{Z} \times \mathbb{Z}_2$	$\mathbb{Z} \times \mathbb{Z}_2$	$(n_{6d}, x_{6d})$

TABLE A15. No. 15,  $p31m$ .

Equivalence relations: Type (i)

$$n_{1a} - 6k, n_{2b} + 3k \quad (\text{B73})$$

$$n_{1a} - 3k, n_{3c} + k \quad (\text{B74})$$

$$n_{1a} - 6k, n_{6d} + k. \quad (\text{B75})$$

Type (ii)

$$-m_{1a}, -m_{3c}. \quad (\text{B76})$$

Reduced indices:

$$(n_{1a}, n_{2b}, n_{3c}, n_{6d}, m_{1a}, m_{3c}) \in (\mathbb{Z})^4 \times (\mathbb{Z}_2)^2 \rightarrow (n_{1a}, n_{2b}, m \equiv m_{1a}m_{3c}) \in (\mathbb{Z}_3)^2 \times \mathbb{Z}_2 \quad (\text{B77})$$

### No. 16 ( $p6$ )

WP	dim	site symm.	$G_{\text{spa}}$	Classification	Gappable decorations	Indices
1a	0D	$C_6$	$\mathbb{Z}_{12}^F$	$\mathbb{Z} \times \mathbb{Z}_2$	$\mathbb{Z} \times \mathbb{Z}_2$	$(n_{1a}, r_{1a})$
2b	0D	$C_3$	$\mathbb{Z}_6^F$	$\mathbb{Z}$	$\mathbb{Z}$	$n_{2b}$
3c	0D	$C_2$	$\mathbb{Z}_4^F$	$\mathbb{Z} \times \mathbb{Z}_2$	$\mathbb{Z} \times \mathbb{Z}_2$	$(n_{3c}, r_{3c})$
6d	2D	$C_1$	$\mathbb{Z}_1$	$\mathbb{Z} \times \mathbb{Z}_2$	$\mathbb{Z} \times \mathbb{Z}_2$	$(n_{6d}, x_{6d})$

TABLE A16. No. 16,  $p6$ .

Equivalence relations: Type (i)

$$n_{1a} - 6k, n_{2b} + 3k \quad (\text{B78})$$

$$n_{1a} - 6k, n_{3c} + 2k \quad (\text{B79})$$

$$n_{1a} - 6k, n_{6d} + k. \quad (\text{B80})$$

Reduced indices:

$$(n_{1a}, n_{2b}, n_{3c}, n_{6d}) \in (\mathbb{Z})^4 \rightarrow (n_{1a}, n_{2b}, n_{3c}) \in \mathbb{Z}_6 \times \mathbb{Z}_3 \times \mathbb{Z}_2 \quad (\text{B81})$$

**No. 17** ( $p6mm$ )

WP	dim	site symm.	$G_{\text{spa}}$	Classification	Gappable decorations	Indices
1a	0D	$C_{6v}$	$\mathbb{Z}_{12}^F \rtimes \mathbb{Z}_4^F \mathbb{Z}_2^F$	$\mathbb{Z} \times \mathbb{Z}_2 \times \mathbb{Z}_2$	$\mathbb{Z} \times \mathbb{Z}_2 \times \mathbb{Z}_2$	$(n_{1a}, r_{1a}, m_{1a})$
2b	0D	$C_{3v}$	$\mathbb{Z}_6^F \rtimes \mathbb{Z}_4^F \mathbb{Z}_2^F$	$\mathbb{Z} \times \mathbb{Z}_2$	$\mathbb{Z} \times \mathbb{Z}_2$	$(n_{2b}, m_{2b})$
3c	0D	$C_{2v}$	$\mathbb{Z}_4^F \rtimes \mathbb{Z}_4^F \mathbb{Z}_2^F$	$\mathbb{Z} \times \mathbb{Z}_2 \times \mathbb{Z}_2$	$\mathbb{Z} \times \mathbb{Z}_2 \times \mathbb{Z}_2$	$(n_{3c}, r_{3c}, m_{3c})$
6d	1D	$C_s$	$\mathbb{Z}_4^F$	$\mathbb{Z} \times \mathbb{Z}_2 \times \mathbb{Z}_2$	$\mathbb{Z} \times \mathbb{Z}_2 \times \mathbb{Z}_2$	$(n_{6d}, m_{6d}, \nu_{6d})$
6e	1D	$C_s$	$\mathbb{Z}_4^F$	$\mathbb{Z} \times \mathbb{Z}_2 \times \mathbb{Z}_2$	$\mathbb{Z} \times \mathbb{Z}_2 \times \mathbb{Z}_2$	$(n_{6e}, m_{6e}, \nu_{6e})$
12f	2D	$C_1$	$\mathbb{Z}_1$	$\mathbb{Z} \times \mathbb{Z}_2$	$\mathbb{Z} \times \mathbb{Z}_2$	$(n_{12f}, x_{12f})$

TABLE A17. No. 17,  $p6mm$ .

Equivalence relations: Type (i)

$$n_{1a} - 6k, n_{2b} + 3k, \quad (\text{B82})$$

$$n_{1a} - 6k, n_{3c} + 2k, \quad (\text{B83})$$

$$n_{1a} - 6k, n_{6d} + k, \quad (\text{B84})$$

$$n_{1a} - 6k, n_{6e} + k, \quad (\text{B85})$$

$$n_{1a} - 12k, n_{12f} + k. \quad (\text{B86})$$

Type (ii)

$$-m_{2b}, -m_{6e} \quad (\text{B87})$$

$$-m_{6e} \quad (\text{B88})$$

$$-m_{6d}. \quad (\text{B89})$$

While  $m_{2b}$ 's sign can be flipped without altering any other index,  $m_{6e}$  and  $m_{6d}$  can be changed individually. Overall, this leads to trivialization of all these three indices.

Reduced indices:

$$(n_{1a}, n_{2b}, n_{3c}, n_{6d}, n_{6e}, n_{12f}, m_{2b}, m_{6e}, m_{6d}) \in \mathbb{Z}^6 \times (\mathbb{Z}_2)^3 \rightarrow (n_{1a}, n_{2b}, n_{3c}) \in \mathbb{Z}_6 \times \mathbb{Z}_3 \times \mathbb{Z}_2 \quad (\text{B90})$$

**Classification of cFSPTs in wallpaper groups with corresponding indices**

Finally, Table A18 shows the classification for cFSPTs, for each of the 17 wallpaper groups in two dimensions.

No.	Wallpaper	Classification	Noninteracting classification	Indices
1	$p1$	$\mathbb{Z} \times \mathbb{Z}_2$	$\mathbb{Z} \times \mathbb{Z}_2$	$(n_{1a}, x_{1a})$
2	$p2$	$\mathbb{Z} \times (\mathbb{Z}_2)^4 \times (\mathbb{Z}_2)^4 \times \mathbb{Z}_2$	$\mathbb{Z} \times (\mathbb{Z}_2)^4 \times \mathbb{Z}_2$	$(n, n_{1a}, n_{1b}, n_{1c}, n_{1d}, r_{1a}, r_{1b}, r_{1c}, r_{1d}, x_{2e})$
3	$p1m1$	$\mathbb{Z} \times (\mathbb{Z}_2)^2 \times (\mathbb{Z}_2)^4 \times \mathbb{Z}_2$	$\mathbb{Z} \times (\mathbb{Z}_2)^2 \times \mathbb{Z}_2$	$(n, n_{1a}, n_{1b}, m_{1a}, m_{1b}, \nu_{1a}, \nu_{1b}, x_{2c})$
4	$p1g1$	$\mathbb{Z} \times \mathbb{Z}_2$	$\mathbb{Z} \times \mathbb{Z}_2$	$(n_{2a}, x_{2a})$
5	$c1m1$	$\mathbb{Z} \times \mathbb{Z}_2 \times (\mathbb{Z}_2)^2 \times \mathbb{Z}_2$	$\mathbb{Z} \times \mathbb{Z}_2 \times \mathbb{Z}_2$	$(n, n_{2a}, m_{2a}, \nu_{2a}, x_{4b})$
6	$p2mm$	$\mathbb{Z} \times (\mathbb{Z}_2)^4 \times (\mathbb{Z}_2)^{12} \times \mathbb{Z}_2$	$\mathbb{Z} \times (\mathbb{Z}_2)^4 \times \mathbb{Z}_2$	$(n, n_{1a}, n_{1b}, n_{1c}, n_{1d}, r_{1a}, m_{1a}, r_{1b}, m_{1b}, r_{1c}, m_{1c}, r_{1d}, m_{1d}, \nu_{2e}, \nu_{2f}, \nu_{2g}, \nu_{2h}, x_{4i})$
7	$p2mg$	$\mathbb{Z} \times (\mathbb{Z}_2)^3 \times (\mathbb{Z}_2)^4 \times \mathbb{Z}_2$	$\mathbb{Z} \times (\mathbb{Z}_2)^3 \times \mathbb{Z}_2$	$(n, n_{2a}, n_{2b}, n_{2c}, r_{2a}, r_{2b}, m_{2c}, \nu_{2c}, x_{4d})$
8	$p2gg$	$\mathbb{Z} \times (\mathbb{Z}_2)^2 \times (\mathbb{Z}_2)^2 \times \mathbb{Z}_2$	$\mathbb{Z} \times (\mathbb{Z}_2)^2 \times \mathbb{Z}_2$	$(n, n_{2a}, n_{2b}, r_{2a}, r_{2b}, x_{4c})$
9	$c2mm$	$\mathbb{Z} \times (\mathbb{Z}_2)^3 \times (\mathbb{Z}_2)^7 \times \mathbb{Z}_2$	$\mathbb{Z} \times (\mathbb{Z}_2)^3 \times \mathbb{Z}_2$	$(n, n_{2a}, n_{2b}, n_{4c}, r_{2a}, m_{2a}, r_{2b}, m_{2b}, r_{4c}, \nu_{4d}, \nu_{4e}, x_{8f})$
10	$p4$	$\mathbb{Z} \times (\mathbb{Z}_4)^2 \times \mathbb{Z}_2 \times (\mathbb{Z}_2)^3 \times \mathbb{Z}_2$	$\mathbb{Z} \times (\mathbb{Z}_4)^2 \times \mathbb{Z}_2 \times \mathbb{Z}_2$	$(n, n_{1a}, n_{1b}, n_{2c}, r_{1a}, r_{1b}, r_{2c}, x_{4d})$
11	$p4mm$	$\mathbb{Z} \times (\mathbb{Z}_4)^2 \times \mathbb{Z}_2 \times (\mathbb{Z}_2)^9 \times \mathbb{Z}_2$	$\mathbb{Z} \times (\mathbb{Z}_4)^2 \times \mathbb{Z}_2 \times \mathbb{Z}_2$	$(n, n_{1a}, n_{1b}, n_{2c}, r_{1a}, m_{1a}, r_{1b}, m_{1b}, r_{2c}, m_{2c}, \nu_{4d}, \nu_{4e}, \nu_{4f}, x_{8g})$
12	$p4gm$	$\mathbb{Z} \times (\mathbb{Z}_4)^2 \times \mathbb{Z}_2 \times (\mathbb{Z}_2)^4 \times \mathbb{Z}_2$	$\mathbb{Z} \times (\mathbb{Z}_4)^2 \times \mathbb{Z}_2 \times \mathbb{Z}_2$	$(n, n_{2a}, n_{2b}, n_{4c}, r_{2a}, r_{2b}, m_{2b}, \nu_{4c}, x_{8d})$
13	$p3$	$\mathbb{Z} \times (\mathbb{Z}_3)^3 \times \mathbb{Z}_2$	$\mathbb{Z} \times (\mathbb{Z}_3)^3 \times \mathbb{Z}_2$	$(n, n_{1a}, n_{1b}, n_{1c}, x_{3d})$
14	$p3m1$	$\mathbb{Z} \times (\mathbb{Z}_3)^3 \times (\mathbb{Z}_2)^2 \times \mathbb{Z}_2$	$\mathbb{Z} \times (\mathbb{Z}_3)^3 \times \mathbb{Z}_2$	$(n, n_{1a}, n_{1b}, n_{1c}, m \equiv m_{1a}m_{1b}m_{1c}m_{3d}, \nu_{3d}, x_{6e})$
15	$p31m$	$\mathbb{Z} \times (\mathbb{Z}_3)^2 \times (\mathbb{Z}_2)^2 \times \mathbb{Z}_2$	$\mathbb{Z} \times (\mathbb{Z}_3)^2 \times \mathbb{Z}_2$	$(n, n_{1a}, n_{2b}, m \equiv m_{1a}m_{3c}, \nu_{3c}, x_{6d})$
16	$p6$	$\mathbb{Z} \times \mathbb{Z}_6 \times \mathbb{Z}_3 \times \mathbb{Z}_2 \times (\mathbb{Z}_2)^2 \times \mathbb{Z}_2$	$\mathbb{Z} \times \mathbb{Z}_6 \times \mathbb{Z}_3 \times \mathbb{Z}_2 \times \mathbb{Z}_2$	$(n, n_{1a}, n_{2b}, n_{3c}, r_{1a}, r_{3c}, x_{6d})$
17	$p6mm$	$\mathbb{Z} \times \mathbb{Z}_6 \times \mathbb{Z}_3 \times \mathbb{Z}_2 \times (\mathbb{Z}_2)^6 \times \mathbb{Z}_2$	$\mathbb{Z} \times \mathbb{Z}_6 \times \mathbb{Z}_3 \times \mathbb{Z}_2 \times \mathbb{Z}_2$	$(n, n_{1a}, n_{2b}, n_{3c}, r_{1a}, m_{1a}, r_{3c}, m_{3c}, \nu_{6d}, \nu_{6e}, x_{12f})$

TABLE A18. Classification of cFSPTs in wallpaper groups. Every wallpaper group has a  $\mathbb{Z}$  factor in its classification due to the total number of Kramers' pairs in the unit-cell (with index  $n$ ), and a  $\mathbb{Z}_2$  factor (with index  $x_{wp}$ , with  $wp$  the general Wyckoff position label) deriving from the intrinsic 2D SPT phase that does not require crystalline symmetries to be realized (colored in magenta). Terms in the classification and indices colored in black correspond to phases that exist both in the absence or presence of interactions. The terms corresponding to intrinsically interacting phases in the classification and their corresponding indices are highlighted in cyan. Note that the "Indices" column refers to the "Classification" column, and the ordering is consistent between the two.

- |   |  |
|---|--|
| <p>[1] A. P. Schnyder, S. Ryu, A. Furusaki, and A. W. W. Ludwig, Classification of Topological Insulators and Superconductors, <i>AIP Conference Proceedings</i> <b>1134</b>, 10 (2009), <a href="https://pubs.aip.org/aip/acp/article-pdf/1134/1/10/11584263/10_1_online.pdf">https://pubs.aip.org/aip/acp/article-pdf/1134/1/10/11584263/10_1_online.pdf</a>.</p> <p>[2] A. Kitaev, Periodic table for topological insulators and superconductors, <i>AIP Conference Proceedings</i> <b>1134</b>, 22 (2009), <a href="https://pubs.aip.org/aip/acp/article-pdf/1134/1/22/11584243/22_1_online.pdf">https://pubs.aip.org/aip/acp/article-pdf/1134/1/22/11584243/22_1_online.pdf</a>.</p> | <p>[3] S. Ryu, A. P. Schnyder, A. Furusaki, and A. W. W. Ludwig, Topological insulators and superconductors: tenfold way and dimensional hierarchy, <i>New Journal of Physics</i> <b>12</b>, 065010 (2010), <a href="https://arxiv.org/abs/0912.2157">arXiv:0912.2157</a> [cond-mat.mes-hall].</p> <p>[4] K. v.Klitzing, G. Dorda, and M. Pepper, New Method for High-Accuracy Determination of the Fine-Structure Constant Based on Quantized Hall Resistance, <i>Phys. Rev. Lett.</i> <b>45</b>, 494 (1980).</p> |
|---|--|



- [5] X. Chen, Z.-C. Gu, and X.-G. Wen, Local unitary transformation, long-range quantum entanglement, wave function renormalization, and topological order, *Phys. Rev. B* **82**, 155138 (2010).
- [6] D. S. Freed and M. J. Hopkins, Reflection positivity and invertible topological phases, *Geometry & Topology* **25**, 1165 (2021).
- [7] B. A. Bernevig, T. L. Hughes, and S.-C. Zhang, Quantum Spin Hall Effect and Topological Phase Transition in HgTe Quantum Wells, *Science* **314**, 1757–1761 (2006).
- [8] M. König, S. Wiedmann, C. Brüne, A. Roth, H. Buhmann, L. W. Molenkamp, X.-L. Qi, and S.-C. Zhang, Quantum Spin Hall Insulator State in HgTe Quantum Wells, *Science* **318**, 766–770 (2007).
- [9] A. Roth, C. Brüne, H. Buhmann, L. W. Molenkamp, J. Maciejko, X.-L. Qi, and S.-C. Zhang, Nonlocal Transport in the Quantum Spin Hall State, *Science* **325**, 294–297 (2009).
- [10] D. Hsieh, D. Qian, L. Wray, Y. Xia, Y. S. Hor, R. J. Cava, and M. Z. Hasan, A topological Dirac insulator in a quantum spin Hall phase (experimental realization of a 3D Topological Insulator) (2009), [arXiv:0910.2420 \[cond-mat.mes-hall\]](https://arxiv.org/abs/0910.2420).
- [11] Y. Xia, D. Qian, D. Hsieh, L. Wray, A. Pal, H. Lin, A. Bansil, D. Grauer, Y. S. Hor, R. J. Cava, and M. Z. Hasan, Observation of a large-gap topological-insulator class with a single Dirac cone on the surface, *Nature Physics* **5**, 398 (2009), [arXiv:0908.3513](https://arxiv.org/abs/0908.3513).
- [12] L. Fu and C. L. Kane, Topological insulators with inversion symmetry, *Phys. Rev. B* **76**, 045302 (2007).
- [13] L. Fu, Topological crystalline insulators, *Phys. Rev. Lett.* **106**, 106802 (2011).
- [14] R.-J. Slager, A. Mesaros, V. Juricic, and J. Zaanen, The space group classification of topological band-insulators, *Nature Physics* **9**, 98 (2013).
- [15] F. Zhang, C. L. Kane, and E. J. Mele, Topological mirror superconductivity, *Phys. Rev. Lett.* **111**, 056403 (2013).
- [16] C.-K. Chiu, H. Yao, and S. Ryu, Classification of topological insulators and superconductors in the presence of reflection symmetry, *Phys. Rev. B* **88**, 075142 (2013).
- [17] T. Morimoto and A. Furusaki, Topological classification with additional symmetries from clifford algebras, *Phys. Rev. B* **88**, 125129 (2013).
- [18] C. Fang, M. J. Gilbert, and B. A. Bernevig, Entanglement spectrum classification of  $C_n$ -invariant noninteracting topological insulators in two dimensions, *Phys. Rev. B* **87**, 035119 (2013).
- [19] P. Jadaun, D. Xiao, Q. Niu, and S. K. Banerjee, Topological classification of crystalline insulators with space group symmetry, *Phys. Rev. B* **88**, 085110 (2013).
- [20] M. Koshino, T. Morimoto, and M. Sato, Topological zero modes and dirac points protected by spatial symmetry and chiral symmetry, *Phys. Rev. B* **90**, 115207 (2014).
- [21] C.-X. Liu, R.-X. Zhang, and B. K. VanLeeuwen, Topological nonsymmorphic crystalline insulators, *Phys. Rev. B* **90**, 085304 (2014).
- [22] K. Shiozaki and M. Sato, Topology of crystalline insulators and superconductors, *Phys. Rev. B* **90**, 165114 (2014).
- [23] Y. Ando and L. Fu, Topological crystalline insulators and topological superconductors: From concepts to materials, *Annual Review of Condensed Matter Physics* **6**, 361 (2015).
- [24] L. Trifunovic and P. Brouwer, Bott periodicity for the topological classification of gapped states of matter with reflection symmetry, *Phys. Rev. B* **96**, 195109 (2017).
- [25] W. A. Benalcazar, B. A. Bernevig, and T. L. Hughes, Electric multipole moments, topological multipole moment pumping, and chiral hinge states in crystalline insulators, *Phys. Rev. B* **96**, 245115 (2017).
- [26] F. Schindler, A. M. Cook, M. G. Vergniory, Z. Wang, S. S. P. Parkin, B. A. Bernevig, and T. Neupert, Higher-order topological insulators, *Science Advances* **4**, 10.1126/sciadv.aat0346 (2018).
- [27] L. Trifunovic and P. W. Brouwer, Higher-Order Bulk-Boundary Correspondence for Topological Crystalline Phases, *Phys. Rev. X* **9**, 011012 (2019).
- [28] C. Fang and L. Fu, New classes of topological crystalline insulators having surface rotation anomaly, *Science Advances* **5**, 10.1126/sciadv.aat2374 (2019).
- [29] Z. Song, Z. Fang, and C. Fang,  $(d - 2)$ -Dimensional Edge States of Rotation Symmetry Protected Topological States, *Phys. Rev. Lett.* **119**, 246402 (2017).
- [30] H. C. Po, A. Vishwanath, and H. Watanabe, Symmetry-based indicators of band topology in the 230 space groups, *Nature Communications* **8**, 10.1038/s41467-017-00133-2 (2017).
- [31] H. C. Po, Symmetry indicators of band topology, *Journal of Physics: Condensed Matter* **32**, 263001 (2020).
- [32] B. Bradlyn, L. Elcoro, J. Cano, M. G. Vergniory, Z. Wang, C. Felser, M. I. Aroyo, and B. A. Bernevig, Topological quantum chemistry, *Nature* **547**, 298 (2017).
- [33] J. Kruthoff, J. de Boer, J. van Wezel, C. L. Kane, and R.-J. Slager, Topological Classification of Crystalline Insulators through Band Structure Combinatorics, *Phys. Rev. X* **7**, 041069 (2017).
- [34] M. Vergniory, L. Elcoro, C. Felser, *et al.*, A complete catalogue of high-quality topological materials, *Nature* **566**, 480–485 (2019).
- [35] J. Cano and B. Bradlyn, Band Representations and Topological Quantum Chemistry, *Annual Review of Condensed Matter Physics* **12**, 225 (2021), <https://doi.org/10.1146/annurev-conmatphys-041720-124134>.
- [36] L. Elcoro, B. J. Wieder, Z. Song, Y. Xu, B. Bradlyn, and B. A. Bernevig, Magnetic topological quantum chemistry, *Nature Communications* **12**, 5965 (2021), [arXiv:2010.00598](https://arxiv.org/abs/2010.00598).
- [37] F. Schindler, Z. Wang, M. G. Vergniory, A. M. Cook, A. Murani, S. Sengupta, A. Y. Kasumov, R. Deblock, S. Jeon, I. Drozdov, H. Bouchiat, S. Guéron, A. Yazdani, B. A. Bernevig, and T. Neupert, Higher-order topology in bismuth, *Nature Physics* **14**, 918–924 (2018).
- [38] t. . P. Chuang-Han Hsu and Xiaoting Zhou and Qiong Ma and Nuh Gedik and Arun Bansil and Vitor M Pereira and Hsin Lin and Liang Fu and Su-Yang Xu and Tay-Rong Chang, *2D Materials* **6**, 031004 (2019).
- [39] C. Yoon, C.-C. Liu, H. Min, and F. Zhang, Quasi-One-Dimensional Higher-Order Topological Insulators (2020), [arXiv:2005.14710 \[cond-mat.mes-hall\]](https://arxiv.org/abs/2005.14710).
- [40] L. Aggarwal, P. Zhu, T. L. Hughes, and V. Madhavan, Evidence for higher order topology in Bi and Bi<sub>0.92</sub>Sb<sub>0.08</sub>, *Nature Communications* **12**,

- [10.1038/s41467-021-24683-8](#) (2021).
- [41] N. Shumiya, M. S. Hossain, J.-X. Yin, Z. Wang, M. Litskevich, C. Yoon, Y. Li, Y. Yang, Y.-X. Jiang, G. Cheng, Y.-C. Lin, Q. Zhang, Z.-J. Cheng, T. A. Cochran, D. Multer, X. P. Yang, B. Casas, T.-R. Chang, T. Neupert, Z. Yuan, S. Jia, H. Lin, N. Yao, L. Balicas, F. Zhang, Y. Yao, and M. Z. Hasan, Evidence of a room-temperature quantum spin Hall edge state in a higher-order topological insulator, *Nature Materials* **21**, 1111 (2022), [arXiv:2110.05718 \[cond-mat.mes-hall\]](#).
  - [42] M. Serra-Garcia, V. Peri, R. Süsstrunk, O. R. Bilal, T. Larsen, L. G. Villanueva, and S. D. Huber, Observation of a phononic quadrupole topological insulator, *Nature (London)* **555**, 342 (2018), [arXiv:1708.05015](#).
  - [43] M. O. Soldini, F. Küster, G. Wagner, S. Das, A. Aldarawshah, R. Thomale, S. Lounis, S. S. P. Parkin, P. Sessi, and T. Neupert, Two-dimensional Shiba lattices as a possible platform for crystalline topological superconductivity, *Nature Physics* **19**, 1848–1854 (2023).
  - [44] H. Wang, P. Fan, J. Chen, L. Jiang, H.-J. Gao, J. L. Lado, and K. Yang, Realizing topological quantum magnets with atomic spins on surfaces (2024), [arXiv:2403.14145 \[cond-mat.mes-hall\]](#).
  - [45] L. Fidkowski and A. Kitaev, Effects of interactions on the topological classification of free fermion systems, *Phys. Rev. B* **81**, 134509 (2010).
  - [46] L. Fidkowski and A. Kitaev, Topological phases of fermions in one dimension, *Phys. Rev. B* **83**, 075103 (2011).
  - [47] S. Ryu and S.-C. Zhang, Interacting topological phases and modular invariance, *Phys. Rev. B* **85**, 245132 (2012).
  - [48] X.-L. Qi, A new class of  $(2 + 1)$ -dimensional topological superconductors with  $\mathbb{Z}_8$  topological classification, *New Journal of Physics* **15**, 065002 (2013).
  - [49] L. Fidkowski, X. Chen, and A. Vishwanath, Non-abelian topological order on the surface of a 3d topological superconductor from an exactly solved model, *Phys. Rev. X* **3**, 041016 (2013).
  - [50] H. Yao and S. Ryu, Interaction effect on topological classification of superconductors in two dimensions, *Phys. Rev. B* **88**, 064507 (2013).
  - [51] M. A. Metlitski, L. Fidkowski, X. Chen, and A. Vishwanath, Interaction effects on 3d topological superconductors: surface topological order from vortex condensation, the 16 fold way and fermionic kramers doublets, [arXiv preprint arXiv:1406.3032](#) (2014).
  - [52] C. Wang and T. Senthil, Interacting fermionic topological insulators/superconductors in three dimensions, *Phys. Rev. B* **89**, 195124 (2014).
  - [53] Y.-Z. You and C. Xu, Symmetry-protected topological states of interacting fermions and bosons, *Phys. Rev. B* **90**, 245120 (2014).
  - [54] T. Morimoto, A. Furusaki, and C. Mudry, Breakdown of the topological classification  $\mathbb{Z}$  for gapped phases of noninteracting fermions by quartic interactions, *Phys. Rev. B* **92**, 125104 (2015).
  - [55] T. Yoshida and A. Furusaki, Correlation effects on topological crystalline insulators, *Phys. Rev. B* **92**, 085114 (2015).
  - [56] X.-Y. Song and A. P. Schnyder, Interaction effects on the classification of crystalline topological insulators and superconductors, *Phys. Rev. B* **95**, 195108 (2017).
  - [57] Ö. M. Aksoy, J.-H. Chen, S. Ryu, A. Furusaki, and C. Mudry, Stability against contact interactions of a topological superconductor in two-dimensional space protected by time-reversal and reflection symmetries, *Phys. Rev. B* **103**, 205121 (2021).
  - [58] X. Chen, Z.-C. Gu, and X.-G. Wen, Classification of gapped symmetric phases in one-dimensional spin systems, *Phys. Rev. B* **83**, 035107 (2011).
  - [59] X. Chen, Z.-C. Gu, and X.-G. Wen, Complete classification of one-dimensional gapped quantum phases in interacting spin systems, *Phys. Rev. B* **84**, 235128 (2011).
  - [60] X. Chen, Z.-X. Liu, and X.-G. Wen, Two-dimensional symmetry-protected topological orders and their protected gapless edge excitations, *Phys. Rev. B* **84**, 235141 (2011).
  - [61] X. Chen, Z.-C. Gu, Z.-X. Liu, and X.-G. Wen, Symmetry protected topological orders and the group cohomology of their symmetry group, *Phys. Rev. B* **87**, 155114 (2013).
  - [62] X. Chen, Y.-M. Lu, and A. Vishwanath, Symmetry-protected topological phases from decorated domain walls, *Nature Communications* **5**, 10.1038/ncomms4507 (2014).
  - [63] A. Kapustin, Symmetry protected topological phases, anomalies, and cobordisms: Beyond group cohomology (2014), [arXiv:1403.1467 \[cond-mat.str-el\]](#).
  - [64] A. Kapustin, Bosonic topological insulators and paramagnets: a view from cobordisms (2014), [arXiv:1404.6659 \[cond-mat.str-el\]](#).
  - [65] Z.-C. Gu and X.-G. Wen, Symmetry-protected topological orders for interacting fermions: Fermionic topological nonlinear  $\sigma$  models and a special group supercohomology theory, *Phys. Rev. B* **90**, 115141 (2014).
  - [66] A. Kapustin, R. Thorngren, A. Turzillo, and Z. Wang, Fermionic symmetry protected topological phases and cobordisms, *Journal of High Energy Physics* **2015**, 1 (2015).
  - [67] Q.-R. Wang and Z.-C. Gu, Construction and classification of symmetry-protected topological phases in interacting fermion systems, *Phys. Rev. X* **10**, 031055 (2020).
  - [68] M. Barkeshli, Y.-A. Chen, P.-S. Hsin, and N. Manjunath, Classification of  $(2+1)$ d invertible fermionic topological phases with symmetry, *Phys. Rev. B* **105**, 235143 (2022).
  - [69] C. Wang, C.-H. Lin, and Z.-C. Gu, Interacting fermionic symmetry-protected topological phases in two dimensions, *Phys. Rev. B* **95**, 195147 (2017).
  - [70] M. Cheng, N. Tantivasadakarn, and C. Wang, Loop braiding statistics and interacting fermionic symmetry-protected topological phases in three dimensions, *Phys. Rev. X* **8**, 011054 (2018).
  - [71] N. Tantivasadakarn and A. Vishwanath, Full commuting projector Hamiltonians of interacting symmetry-protected topological phases of fermions, *Phys. Rev. B* **98**, 165104 (2018).
  - [72] J. Sullivan and M. Cheng, Interacting edge states of fermionic symmetry-protected topological phases in two dimensions, *SciPost Phys.* **9**, 016 (2020).
  - [73] M. Cheng and C. Wang, Rotation symmetry-protected topological phases of fermions, *Phys. Rev. B* **105**, 195154 (2022).
  - [74] R. Thorngren and D. V. Else, Gauging spatial symmetries and the classification of topological crystalline phases, *Phys. Rev. X* **8**, 011040 (2018).

- [75] D. V. Else and R. Thorngren, Crystalline topological phases as defect networks, *Phys. Rev. B* **99**, 115116 (2019).
- [76] D. S. Freed and M. J. Hopkins, Invertible phases of matter with spatial symmetry (2019), [arXiv:1901.06419 \[math-ph\]](#).
- [77] A. Debray, Invertible phases for mixed spatial symmetries and the fermionic crystalline equivalence principle (2021), [arXiv:2102.02941 \[math-ph\]](#).
- [78] H. Song, S.-J. Huang, L. Fu, and M. Hermele, *Topological Phases Protected by Point Group Symmetry*, *Phys. Rev. X* **7**, 011020 (2017).
- [79] S.-J. Huang, H. Song, Y.-P. Huang, and M. Hermele, *Building crystalline topological phases from lower-dimensional states*, *Phys. Rev. B* **96**, 205106 (2017).
- [80] J.-H. Zhang, Q.-R. Wang, S. Yang, Y. Qi, and Z.-C. Gu, Construction and classification of point-group symmetry-protected topological phases in two-dimensional interacting fermionic systems, *Phys. Rev. B* **101**, 100501(R) (2020).
- [81] J.-H. Zhang, Y. Qi, and Z.-C. Gu, Construction and classification of crystalline topological superconductor and insulators in three-dimensional interacting fermion systems, [arXiv e-prints](#), [arXiv:2204.13558 \(2022\)](#), [arXiv:2204.13558 \[cond-mat.str-el\]](#).
- [82] J.-H. Zhang, S. Yang, Y. Qi, and Z.-C. Gu, *Real-space construction of crystalline topological superconductors and insulators in 2D interacting fermionic systems*, *Phys. Rev. Res.* **4**, 033081 (2022).
- [83] A. Rasmussen and Y.-M. Lu, Intrinsically interacting topological crystalline insulators and superconductors (2018), [arXiv:1810.12317 \[cond-mat.str-el\]](#).
- [84] A. Rasmussen and Y.-M. Lu, Classification and construction of higher-order symmetry-protected topological phases of interacting bosons, *Phys. Rev. B* **101**, 085137 (2020).
- [85] N. Manjunath, V. Calvera, and M. Barkeshli, Characterization and classification of interacting (2+1)D topological crystalline insulators with orientation-preserving wallpaper groups (2023), [arXiv:2309.12389 \[cond-mat.str-el\]](#).
- [86] I.-D. Potirniche, A. C. Potter, M. Schleier-Smith, A. Vishwanath, and N. Y. Yao, Floquet Symmetry-Protected Topological Phases in Cold-Atom Systems, *Phys. Rev. Lett.* **119**, 123601 (2017).
- [87] P. Sompet, S. Hirthe, D. Bourgund, T. Chalopin, J. Bibo, J. Koepsell, P. Bojović, R. Verresen, F. Pollmann, G. Salomon, C. Gross, T. A. Hilker, and I. Bloch, Realizing the symmetry-protected Haldane phase in Fermi-Hubbard ladders, *Nature (London)* **606**, 484 (2022), [arXiv:2103.10421 \[cond-mat.quant-gas\]](#).
- [88] R. Kobayashi, Y. Zhang, Y.-Q. Wang, and M. Barkeshli, (2+1)D topological phases with RT symmetry: many-body invariant, classification, and higher order edge modes (2024), [arXiv:2403.18887 \[cond-mat.str-el\]](#).
- [89] T. Hahn, H. Arnold, M. I. Aroyo, E. F. Bertraut, Y. Biliet, M. J. Buerger, H. Burzlaff, J. D. H. Donnay, W. Fischer, D. S. Fokkema, B. Gruber, H. Klapper, E. Koch, P. B. Konstantinov, G. A. Langlet, A. Looijenga-Vos, U. Müller, P. M. De Wolff, H. Wondratschek, and H. Zimmermann, *International Tables for Crystallography, Vol. A, Space-Group Symmetry*, edited by T. Hahn, Vol. A (Springer, 2005).
- [90] Z. Song, S.-J. Huang, Y. Qi, C. Fang, and M. Hermele, *Topological states from topological crystals*, *Science Advances* **5**, 10.1126/sciadv.aax2007 (2019).
- [91] H. Yao and S. A. Kivelson, Fragile Mott Insulators, *Physical Review Letters* **105**, 166402 (2010).
- [92] A. Turzillo and M. You, Fermionic matrix product states and one-dimensional short-range entangled phases with antiunitary symmetries, *Phys. Rev. B* **99**, 035103 (2019).
- [93] C. Bourne and Y. Ogata, The classification of symmetry protected topological phases of one-dimensional fermion systems, *Forum of Mathematics, Sigma* **9**, e25 (2021).
- [94] Ö. M. Aksoy and C. Mudry, Elementary derivation of the stacking rules of invertible fermionic topological phases in one dimension, *Phys. Rev. B* **106**, 035117 (2022).
- [95] C. L. Kane and E. J. Mele,  $\mathbb{Z}_2$  Topological Order and the Quantum Spin Hall Effect, *Physical Review Letters* **95**, 10.1103/physrevlett.95.146802 (2005).
- [96] D. J. Scalapino and S. A. Trugman, Local antiferromagnetic correlations and  $d_{x^2-y^2}$  pairing, *Philosophical Magazine B* **74**, 607 (1996), <https://doi.org/10.1080/01418639608240361>.
- [97] S. Chakravarty and S. A. Kivelson, Electronic mechanism of superconductivity in the cuprates,  $C_{60}$ , and polyacenes, *Phys. Rev. B* **64**, 064511 (2001).
- [98] R. Schumann, Thermodynamics of a 4-site Hubbard model by analytical diagonalization, *Annalen der Physik* **11**, 49 (2002).
- [99] L. Muechler, J. Maciejko, T. Neupert, and R. Car, Möbius molecules and fragile Mott insulators, *Phys. Rev. B* **90**, 245142 (2014).
- [100] M. O. Soldini, N. Astrakhantsev, M. Iraola, A. Tiwari, M. H. Fischer, R. Valentí, M. G. Vergniory, G. Wagner, and T. Neupert, Interacting topological quantum chemistry of Mott atomic limits, *Physical Review B* **107**, 245145 (2023).
- [101] J. Herzog-Arbeitman, A. Bernevig, and Z. Song, Interacting topological quantum chemistry in 2D with many-body real space invariants, *Nature Communications*, **1171** (2024).
- [102] M. Suzuki, Relationship among Exactly Soluble Models of Critical Phenomena. I\*): 2D Ising Model, Dimer Problem and the Generalized XY-Model, *Progress of Theoretical Physics* **46**, 1337 (1971), <https://academic.oup.com/ptp/article-pdf/46/5/1337/5268367/46-5-1337.pdf>.
- [103] W. Son, L. Amico, R. Fazio, A. Hamma, S. Pascazio, and V. Vedral, Quantum phase transition between cluster and antiferromagnetic states, *EPL (Europhysics Letters)* **95**, 50001 (2011).
- [104] R. Verresen, R. Moessner, and F. Pollmann, One-dimensional symmetry protected topological phases and their transitions, *Phys. Rev. B* **96**, 165124 (2017).
- [105] M. Iraola, N. Heinsdorf, A. Tiwari, D. Lessnich, T. Mertz, F. Ferrari, M. H. Fischer, S. M. Winter, F. Pollmann, T. Neupert, R. Valentí, and M. G. Vergniory, Towards a topological quantum chemistry description of correlated systems: The case of the hubbard diamond chain, *Phys. Rev. B* **104**, 195125 (2021).
- [106] V. Gurarie, Single-particle Green's functions and interacting topological insulators, *Phys. Rev. B* **83**, 085426 (2011).

- [107] Z. Wang, X.-L. Qi, and S.-C. Zhang, Topological invariants for interacting topological insulators with inversion symmetry, *Phys. Rev. B* **85**, 165126 (2012).
- [108] Z. Wang and B. Yan, Topological Hamiltonian as an exact tool for topological invariants, *Journal of Physics: Condensed Matter* **25**, 155601 (2013).
- [109] D. Lessnich, S. M. Winter, M. Iraola, M. G. Vergniory, and R. Valentí, Elementary band representations for the single-particle Green's function of interacting topological insulators, *Physical Review B* **104**, 085116 (2021).
- [110] W. A. Benalcazar, T. Li, and T. L. Hughes, Quantization of fractional corner charge in  $C_n$ -symmetric higher-order topological crystalline insulators, *Phys. Rev. B* **99**, 245151 (2019).
- [111] F. Schindler, M. Brzezińska, W. A. Benalcazar, M. Iraola, A. Bouhon, S. S. Tsirkin, M. G. Vergniory, and T. Neupert, Fractional corner charges in spin-orbit coupled crystals, *Phys. Rev. Res.* **1**, 033074 (2019).
- [112] Y. Fang and J. Cano, Filling anomaly for general two- and three-dimensional  $C_4$  symmetric lattices, *Phys. Rev. B* **103**, 165109 (2021).
- [113] D. Pérez-García, M. M. Wolf, M. Sanz, F. Verstraete, and J. I. Cirac, String order and symmetries in quantum spin lattices, *Phys. Rev. Lett.* **100**, 167202 (2008).
- [114] F. Pollmann, E. Berg, A. M. Turner, and M. Oshikawa, Symmetry protection of topological phases in one-dimensional quantum spin systems, *Phys. Rev. B* **85**, 075125 (2012).
- [115] F. Pollmann and A. M. Turner, Detection of symmetry-protected topological phases in one dimension, *Phys. Rev. B* **86**, 125441 (2012).
- [116] H. Shapourian, K. Shiozaki, and S. Ryu, Many-body topological invariants for fermionic symmetry-protected topological phases, *Phys. Rev. Lett.* **118**, 216402 (2017).
- [117] K. Shiozaki, H. Shapourian, K. Gomi, and S. Ryu, Many-body topological invariants for fermionic short-range entangled topological phases protected by antiunitary symmetries, *Phys. Rev. B* **98**, 035151 (2018).
- [118] Y. Zhang, N. Manjunath, R. Kobayashi, and M. Barkeshli, Complete crystalline topological invariants from partial rotations in (2+1)D invertible fermionic states and Hofstadter's butterfly (2023), [arXiv:2303.16919 \[cond-mat.str-el\]](https://arxiv.org/abs/2303.16919).
- [119] E. Lieb, T. Schultz, and D. Mattis, Two soluble models of an antiferromagnetic chain, *Annals of Physics* **16**, 407 (1961).
- [120] M. Oshikawa, Commensurability, excitation gap, and topology in quantum many-particle systems on a periodic lattice, *Phys. Rev. Lett.* **84**, 1535 (2000).
- [121] M. B. Hastings, Lieb-schultz-mattis in higher dimensions, *Phys. Rev. B* **69**, 104431 (2004).
- [122] M. B. Hastings, Sufficient conditions for topological order in insulators, *Europhysics Letters (EPL)* **70**, 824 (2005).
- [123] M. Cheng, M. Zaletel, M. Barkeshli, A. Vishwanath, and P. Bonderson, Translational symmetry and microscopic constraints on symmetry-enriched topological phases: A view from the surface, *Phys. Rev. X* **6**, 041068 (2016).
- [124] G. Y. Cho, C.-T. Hsieh, and S. Ryu, Anomaly manifestation of lieb-schultz-mattis theorem and topological phases, *Phys. Rev. B* **96**, 195105 (2017).
- [125] H. Tasaki, Lieb-schultz-mattis theorem with a local twist for general one-dimensional quantum systems, *Journal of Statistical Physics* **170**, 653 (2018).
- [126] C.-M. Jian, Z. Bi, and C. Xu, Lieb-schultz-mattis theorem and its generalizations from the perspective of the symmetry-protected topological phase, *Phys. Rev. B* **97**, 054412 (2018).
- [127] Y. Ogata and H. Tasaki, Lieb-Schultz-Mattis type theorems for quantum spin chains without continuous symmetry, *Communications in Mathematical Physics* **372**, 951 (2019).
- [128] Y. Ogata, Y. Tachikawa, and H. Tasaki, General Lieb-Schultz-Mattis Type Theorems for Quantum Spin Chains, *Communications in Mathematical Physics* **385**, 79 (2021).
- [129] Y. Yao and M. Oshikawa, Twisted Boundary Condition and Lieb-Schultz-Mattis Inapplicability for Discrete Symmetries, *Phys. Rev. Lett.* **126**, 217201 (2021).
- [130] Ö. M. Aksoy, A. Tiwari, and C. Mudry, Lieb-Schultz-Mattis type theorems for Majorana models with discrete symmetries, *Phys. Rev. B* **104**, 075146 (2021).
- [131] H. C. Po, H. Watanabe, and A. Vishwanath, Fragile Topology and Wannier Obstructions, *Phys. Rev. Lett.* **121**, 126402 (2018).
- [132] B. Bradlyn, Z. Wang, J. Cano, and B. A. Bernevig, Disconnected elementary band representations, fragile topology, and Wilson loops as topological indices: An example on the triangular lattice, *Phys. Rev. B* **99**, 045140 (2019).
- [133] A. Bouhon, A. M. Black-Schaffer, and R.-J. Slager, Wilson loop approach to fragile topology of split elementary band representations and topological crystalline insulators with time-reversal symmetry, *Phys. Rev. B* **100**, 195135 (2019).
- [134] D. V. Else, H. C. Po, and H. Watanabe, Fragile topological phases in interacting systems, *Phys. Rev. B* **99**, 125122 (2019).
- [135] M. I. Aroyo, J. M. Perez-Mato, C. Capillas, E. Kroumova, S. Ivantchev, G. Madariaga, A. Kirov, and H. Wondratschek, Bilbao Crystallographic Server: I. Databases and crystallographic computing programs, *Zeitschrift für Kristallographie - Crystalline Materials* **221**, 15 (2006).
- [136] M. I. Aroyo, A. Kirov, C. Capillas, J. M. Perez-Mato, and H. Wondratschek, Bilbao Crystallographic Server. II. Representations of crystallographic point groups and space groups, *Acta Crystallographica Section A* **62**, 115 (2006).
- [137] M. Aroyo, J. Perez-Mato, D. Orobengoa, E. Tasci, G. De La Flor, and A. Kirov, Crystallography online: Bilbao crystallographic server, *Bulgarian Chemical Communications* **43**, 183 – 197 (2011).